INTERFEROMETRIC STUDIES

ON CURVED THIN FILMS

Thesis submitted to the
University of London for the
Degree of Doctor of Philosophy

by

N. Barakat.

Royal Holloway College.

May, 1951.

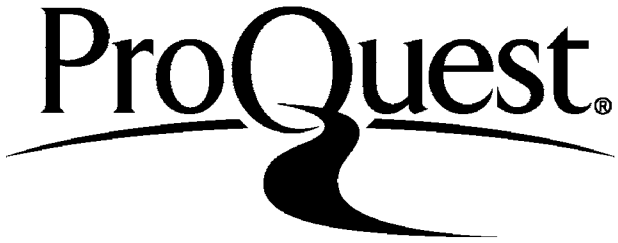

CONTENTS

The following two papers are enclosed in a pocket at the end of the tnesis.

(1). Tolansky and Barakat, Proc. Phys. Soc., 63, 545 (1950)

(2) Barakat, Nature, 16, 603 (1949)

Introduction

If we consider the general case of two intersecting spherical surfaces of different radii of curvature, then as each of the radii of curvature increases without limit along the line joining the centre of the corresponding sphere to a fixed point on the line of intersection, the two intersecting surfaces tend in the limit to two planes forming a wedge.

If one of the radii of curvature increases without limit and the other remains constant, the first surface tends to a plane and we have the case of an interferometer consisting of a plane and a spherical surface. A lens-plate interferometer is a special case when the plane is tangential to the spherical surface.

An arbitrary surface and a plane could be considered to be an extension of the previous simple case.

If the two spherical surfaces are concentric, we have a spherically curved thin film of uniform thickness, a central section through which is identical with the section perpendicular to the axis of a cylindrically curved thin film. As the radii of curvature increase without limit, the interferometer tends to two plane

parallel surfaces.

By evaporating a highly reflecting semi transparent metallic film on both components of these interferometers, multiple beam interference fringes are obtained. Their intensity distribution approaches a Fabry-Perot distribution with the result that there is extreme sharpness of the fringes.

Localization arises from the difference in angles of emergence of the beams leaving the two sides of the interferometer. This depends on the difference in angles of incidence at the first and second surfaces of the interferometer. In the case of a wedge, for incident parallel light, the angles of incidence at the first and second surfaces are constant and their difference is equal to the wedge angle α. The interferometer gap t varies along the wedge. It satisfies the linear relation $t = y \tan \alpha$ where y is the distance measured from the apex along one of the components. In the case of a lens-plate interferometer, a slight variation in the angle of incidence occurs along the curved surface. The interferometer gap t is related to y by the second order equation $t^2 - 2Rt = y^2$. For cylindrically

curved thin films, the angles of incidence at both surfaces vary from nearly $-\frac{\pi}{2}$ to $+\frac{\pi}{2}$, while their difference as well as the interferometer gap remain constant.

Tolansky (1) applied and developed multiple beam interference to both the cases of a lens-plate and an arbitrary surface plate interferometers. The latter is case of Fizeau fringes.

The present work deals with the theory of formation and properties of localized fringes obtained by cylindrically curved thin films. Their application to isotropic, uniaxial and biaxial media is considered in detail.

CHAPTER I

THE INTENSITY DISTRIBUTION OF THE TRANSMITTED AND REFLECTED SYSTEMS FOR PLANE PARALLEL THIN FILMS

Airy (2) has applied the principle of superposition discovered by Young in 1801, to the case of multiple beam interference in a film of uniform thickness.

Considering phase changes at reflection, the expressions for the transmitted and reflected systems are obtained as follows:

Let A and B represent two plane parallel surfaces of an isotropic dielectric medium of thickness t and refractive index μ, coated with identical highly reflecting semi-transparent metallic layers, and let plane wavefronts of wavelength λ fall at any of the surfaces A and B. If T and R are the fractions of light intensity transmitted and reflected at each layer, then the amplitudes are proportional to the square roots of these fractions.

Consider a plane wavefront W of unit amplitude making an angle θ with A and represented by YA_1 the normal to the wavefront (Fig. 1). At A_1 part of the wavefront is reflected along A_1Y_1 and part is transmitted along A_1B_1. At B_1, B_1X_1 and B_1A_2 are transmitted and reflected respectively. Thus by multiple reflections there occur a series of reflected wavefronts represented

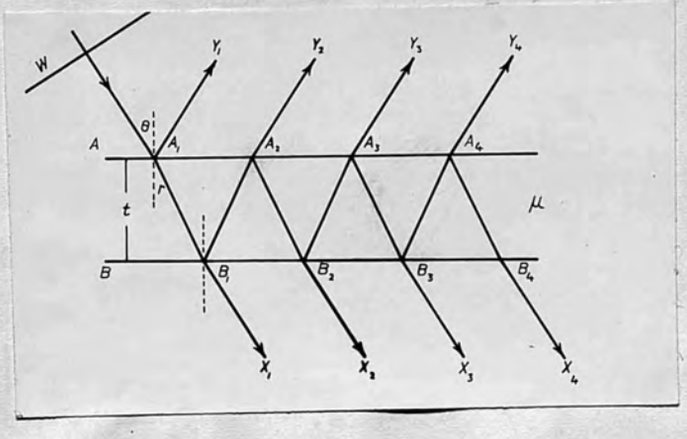

Fig. 1.

by A_1Y_1, A_2Y_2, ... and a series of transmitted wavefronts represented by B_1X_1, B_2X_2, ... Let it be assumed that there occur changes of phase on reflection as well as on transmission through the highly reflecting metallic layers and let it be represented by

β change of phase at reflection med./metallic layer

β_1 " " " " " Air /metallic layer

and γ " " " on transmission through the highly reflecting metallic layers.

The transmitted system

The transmitted rays B_1X_1, B_2X_2, ... are of decreasing amplitude, with a constant phase difference between any two successive rays given by

$$\delta = (2\mu t\cos r) + 2\beta \qquad \text{.....(1)}$$

If e^{iwt} represent the incident light where $\frac{2\pi}{\omega}$ is the frequency then the instantaneous resultant displacement is

$$R_T = Te^{i(wt + 2\gamma)} + TRe^{i(wt + 2\gamma - \delta)} + TR^2e^{i(wt-2\gamma-2\delta)} + ...$$

$$= \frac{T}{1-Re^{-i\delta}} . e^{i(wt + 2\gamma)}$$

$$= A_T\, e^{i(wt + 2\gamma + \Delta_t)}$$

where A_T is the amplitude of the resultant and Δ_t is its phase difference with respect to the first transmitted beam.

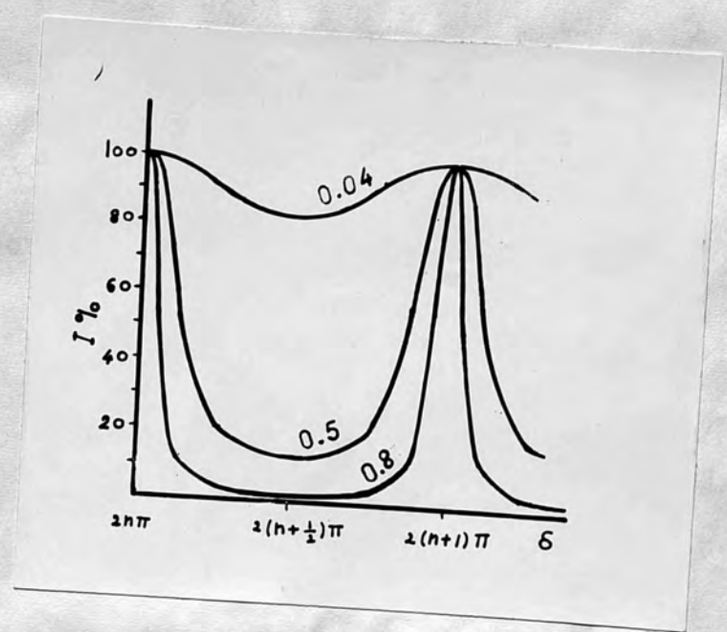

FIG. 2.

$$A_T^2 = I_T = \frac{T^2}{(1-2R\cos\delta + R^2)} = \frac{T^2}{(1-R)^2} \cdot \frac{1}{1 + \frac{4R}{(1-R)^2}\sin^2\delta/2}$$

$$= \frac{T^2}{(1-R)^2} \frac{1}{(1 + F\sin^2\delta/2)} \quad (2)$$

where F is Fabry's coefficient of finesse

As δ varies, I_T assumes different values and is maximum for $\delta = 2n\pi$ and minimum for

$$\delta = (2n + 1)\pi$$

$$I_{max} = \frac{T^2}{(1-R)^2} \qquad \text{and } I_{min} = \frac{T^2}{(1+R)^2}$$

The variation of δ takes place if r, λ or t vary according to equation (1), in the first two cases there is a corresponding variation in β.

In order to show the effect of the reflectivity of the metallic layer on the sharpness of the fringes equation (2) is represented diagramatically in Fig. 2 for R = 80%, 50% and 4% neglecting for the moment the absorption of the layer.

It is clear that any point on the intensity distribution curve is a result of the superposition of an infinite number of beams with a constant phase difference varying from one point to another, where

$$2n\pi \leq \delta \leq 2(n+1)\pi \qquad n = 0,1,2, \ldots\ldots$$

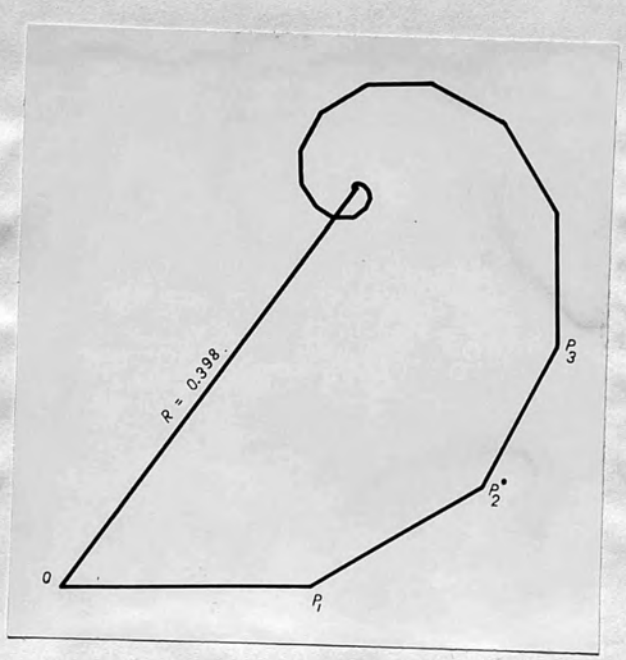

Fig. 3.

In the case of $\delta = 2n\pi$, the beams are in phase, contributing the point of peak intensity on the curve. As δ deviates from this value, the resultant amplitude of the infinite number of beams, with the new phase difference is less than the resultant amplitude at zero phase. In fact it is equal to the square root of the intensity coordinate at the point corresponding to the new phase difference. While the resultant amplitude in the case of $\delta = 2n\pi$ is the algebraic sum of the individual components and thus independent of the reflectivity, it decreases as R increases when the phase difference is an intermediate value between two maxima. Applying the polygon of displacements to the infinite number of beams with phase difference $\delta = 2\pi n \pm \frac{\pi}{6}$ at R = 80%, a spiral shown in Fig. 3 is obtained and the resultant amplitude equals 0.398 of the initial amplitude. Equation (2) gives $I_{80\%} = 0.157$, A = 0.398; the coefficient of finesse = 80. For 50% reflectivity $I_{50\%} = 0.651$, A = 0.807 and F = 8. In fact the result of increasing the reflectivity is merely a more even distribution of intensity among the multiple beams; in other words, the number of beams

of amplitudes more than 1/100 of the first beam, which might be termed the effective beams, increases with R. The profound change in appearance of the interference fringes in transmission and in reflection, when the reflecting coefficient is increased considerably above the value 0.04 characteristic of glass at normal incidence, was pointed out by Boulouch [3]. But it was Fabry and Perot [4] who established the importance of this fact, and who applied it to the measurement of standard wavelengths by using the famous Fabry-Perot interferometer in 1906.

While, strictly speaking, multiple reflections occur in the case of uncoated thin films, the successive amplitudes of the multiple reflected beams die down very quickly. In this case it is practically sufficient to consider the first two beams only and the term two-beams interference fringes is used to distinguish them from the sharp fringes resulting from multiple reflections at coated interferometers. The validity of this terminolcgy is easily seen in the reflected system, because the first two beams for R = 0.04 are the only effective beams and are of nearly the

same amplitude. Thus the intensity distribution curve is approximately $\cos^2 \delta/2$. In the case of the transmitted system, a considerable drop in amplitude takes place after the first transmitted beam, and to obtain a complementary intensity distribution curve more than two beams are summed.

Despite the early realization of the importance of multiple beams, it was only confined to interferometric gaps of uniform thickness. It was due to Tolansky[5] in 1945 to apply and develop the multiple-beam interferometer using non-uniform gaps, thus rendering the two-beam interference fringes an accurate tool for precision work.

The Effect of Absorption

Considering the absorption A of the metallic layer, then $R + T + A = 1$

$$I_{max} = \frac{T^2}{(T + A)^2} = \frac{1}{(1 + \frac{A}{T})^2}$$

and $$I_{min} = \frac{T^2}{(2 - (T + A))^2}$$

A film could be defined by any two of its optical properties R, T and A. Now in deriving equation (2), the amplitude of the components are obtained in terms of both T and R. Thus the same equation accounts for absorption. The graphical presentation in Fig. 2 is obtained on the assumption that $A = 0$ and $T = 1 - R$

Consequently I_T (for $A = 0$) $= \dfrac{1}{1 + \dfrac{4R}{(1 - R)^2} \sin^2 \delta/2}$

and $I_{max} = 1$

Now if the absorption is considered then $T + A = 1 - R$ and the transmissivity T for a certain reflectivity R is reduced by an amount equal to A. Therefore

$$I_T \text{ (for } A \neq o) = \frac{T^2}{(1 - R)^2} \cdot I_T \text{ (for } A = o)$$

$$= \frac{1}{(1 + \frac{A}{T})^2} \cdot I_T \text{ (for } A = o)$$

As δ varies from $2n\pi$ to $2(n + 1)\pi$, the intensity distribution curve for I_T with absorption, is deduced from the ideal curve of I_T for $A = 0$ by multiplying the intensity coordinate of any point on the latter by the fraction $\dfrac{1}{(1 + \frac{A}{T})^2}$. This factor, which like R depends upon the wavelength

and the angle of incidence, could be considered a constant between any two successive fringes. For $R = 0.7$, this factor, which is clearly equal to the peak intensity, increases as R decreases, and the resulting curve is closer to the ideal one, the lower the value of R.

Fig. 4 shows the intensity distribution curve in the ideal case of no absorption for $R = .080$, and the related curve for the same reflectivity $R = 0.80$ and absorption $A = 0.035$. The factor $(1 + \frac{A}{T})^{-2}$ is equal to 0.68. While the drop in the peak intensity is 0.32, the minimum intensity drop is only 0.0039. The two curves become closer and closer as δ approaches the value $(2n + 1)\pi$.

It is important to mention that any property of the fringes in transmission, measured by a quantity which by definition effectively cancels the factor $(1 + \frac{A}{T})^{-2}$, leads to an expression for this property depending only on R and lacking the effect of absorption.

<u>The visibility and half-width of the fringes in transmission</u>

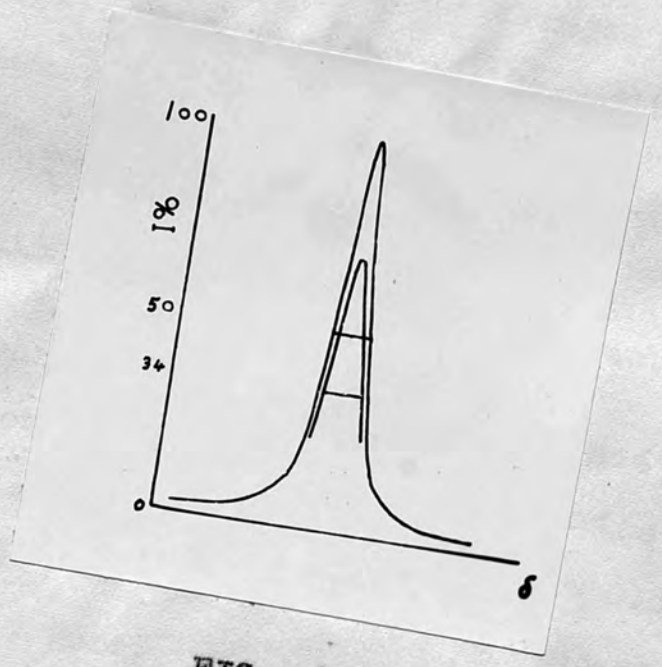

FIG. 4.

If Fizeau's definition of the visibility V is adopted

$$V = \frac{I_{max} - I_{min}}{I_{max} + I_{min}} \quad \text{then} \quad V = \frac{2R}{(1 + R)^2}$$

relating the visibility to the reflectivity only and considering the two curves shown in Fig. 4 to be of the same visibility.

If the sharpness of the fringes is measured by the half-width W, defined as the width at half the peak intensity, then

$$I/I_{max} = \frac{1}{1 + F \sin^2 \delta/2} = \frac{1}{2}$$

$$W = 2\delta = \frac{2(1 - R)}{\sqrt{R}} = \frac{(1 - R)}{\pi\sqrt{R}}$$ as a fraction of an order.

It is clear from the last expression and from Fig. 4 the independence of the half-width on the absorption A, for the same reflectivity. For R = 0.80, W is equal to 1/14 of the separation between any two successive orders.

If the quantity $(I_{max} - I_{min})$ is adopted as a measure of the contrast, it leads to the expression $\frac{T^2}{(1 - R)^2} \left(1 - \left(\frac{1 - R}{1 + R}\right)^2\right)$ which is a function of R and A. Fig. 5 represents diagrammatically the last expression.

Values of R, T and A given by Tolansky (6) are tabulated on page (98).

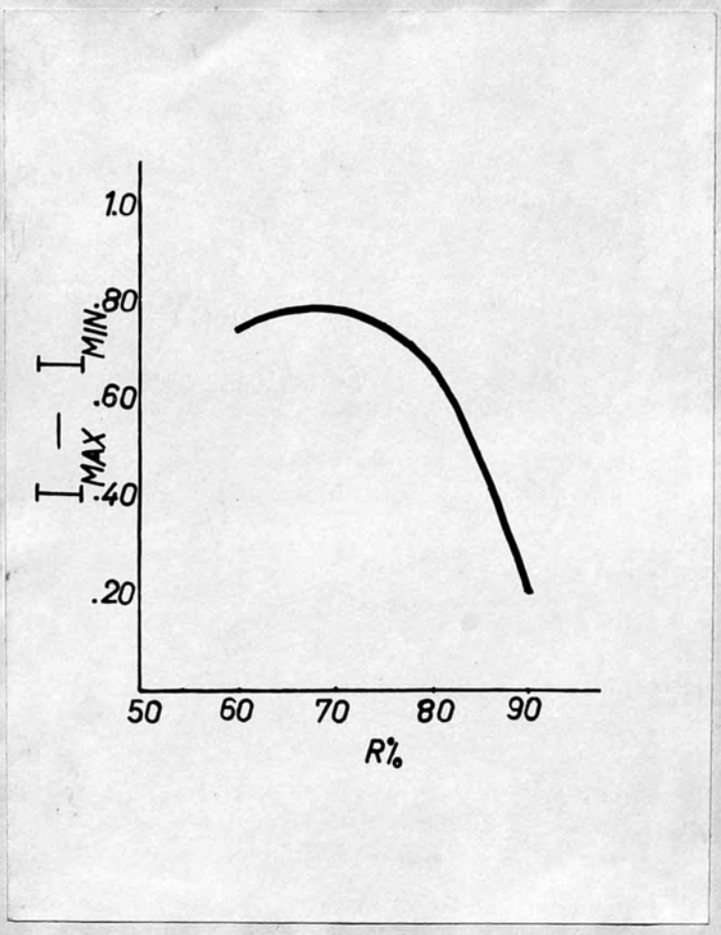

FIG. 5.

The Reflected System

The theory of the reflected system was given by Hamy[7] as early as 1906. In Fig. (1) the system of reflected wavefronts is represented by

A_1Y_1, A_2Y_2, ...

The phase difference between the first and the second beams A_1Y_1 and A_2Y_2 is

$$= 2\gamma - \beta_1 + \beta + \frac{2\pi}{\lambda}(2\mu t \cos r)$$

$$= F + \delta$$

where $F = 2\gamma - (\beta_1 + \beta)$ and $\delta = \frac{2\pi}{\lambda}(2\mu t \cos r) + 2\beta$

The resultant of the reflected wavefronts is equal to

$$\sqrt{R}\, e^{i(wt-\beta_1)} \left\{1 + Te^{-i(\delta+F)} + TRe^{-i(2\delta+F)} + TR^2e^{-i(3\delta+F)} + \cdots\right\}$$

$$= \sqrt{R}\, e^{i(wt-\beta_1)} \cdot \left\{\frac{1 + Te^{-i(\delta+F)}(1 - Re^{i\delta})}{(1 - Re^{-i\delta})(1 - Re^{i\delta})}\right\}$$

Therefore $$I_R = R\left\{1 + \frac{T^2 + 2T\cos(\delta+F) - 2TR\cos F}{1 - 2R\cos\delta + R^2}\right\} \ldots (3)$$

Equation (3) gives an expression for the intensity I_R of the reflected system in terms of R, T, δ and F. From the relation $F = 2\gamma - (\beta_1 + \beta)$ it is clear that F depends only on the first surface, since the change of phase at reflection at the second surface is included only in δ. As δ varies I_R assumes different values. Assuming that the variation in F, R and T could be neglected between

any two successive fringes, the values of δ at which I_R is maximum and minimum are obtained by equating $\frac{dI_R}{d\delta}$ to zero. Thus $M \sin \delta + N \cos \delta = P$

where $M = (1 - R^2) \cos F + RT$ ....(4)

$N = (1 + R^2) \sin F$ ....(5)

$P = 2R \sin F$ ....(6)

putting $\cos Q = \frac{M}{\sqrt{M^2 + N^2}}$, $\sin Q = \frac{N}{\sqrt{N^2 + M^2}}$

and $\sin \psi = \frac{P}{\sqrt{M^2 + N^2}}$ we have

$\sin (\delta + Q) = \sin \psi$ and the solution is

$\delta + Q = l\pi + (-1)^l \psi$ l is an integer

Depending upon whether l is odd or even, δ takes the values $((2n+1)\pi - \phi - \psi)$ or $(2n\pi - \phi + \psi)$. These are the two values of δ at which I_R is maximum and minimum. It is clear that I_R is a periodic function of δ, but any minimum does not occur half way between the two neighbouring maxima. The condition for a minimum to be equidistant to the neighbouring maxima is that

$\psi = 0$ Therefore $P = 2R \sin F = 0$

and $F = K\pi$ K is an integer

Substituting in (5) gives Q to be a multiple of 2π and depending upon whether K is odd or even we have

$2\gamma - (\beta + \beta_1) = 2m\pi$

or $2\gamma - (\beta + \beta_1) = (2m + 1)\pi$

Therefore the two cases are

(1) $F = 2m\pi$ From equation (3)

$$I_R = R\left\{1 + \frac{T^2 - 2T\cos\delta - 2RT}{1 - 2R\cos\delta + R^2}\right\} = I_{max}$$

for

$\delta = 2n\pi$ $\quad I_R = R\left\{1 + \frac{T^2 - 2T - 2RT}{1 - 2R + R^2}\right\} = I_{max}$

for $\delta = (2n+1)\pi$ $\quad I_R = R\left\{1 - \frac{T^2 - 2T - 2RT}{1 - 2R + R^2}\right\} = I_{min}$

(2) $F = 2(m + 1)\pi$

$$I_R = R\left\{1 + \frac{T^2 - 2T\cos\delta + 2RT}{1 - 2R\cos\delta + R^2}\right\}$$

for

$\delta = 2n\pi$

$$I_R = R\left\{1 + \frac{T^2 - 2T + 2RT}{1 - 2R + R^2}\right\} = R\left(1 - \frac{T}{1-R}\right)^2$$

and for $\delta = (2n+1)\pi$ $\quad = I_{min}$

$$I_R = R\left(1 + \frac{T}{1 + R}\right)^2 = I_{min}$$

The last case is of symmetrical dark lines on a bright background which is very nearly the case for high reflectivity. The intensity distribution for $R = .85$ is represented in Fig. (6).

Thus F is very nearly equal to $(2m + 1)\pi$ for $R > 0.7$, Holden[8]. This implies that if F is taken to be equal to $(2m + 1)\pi$, (the minimum intensity $(2m + 1)$), the minimum intensity for the reflected system occurs at the maximum of the transmitted system, the corresponding value for δ is given by $\delta = \frac{2\pi}{\lambda}(2\mu t\cos r) + 2B$

$= 2n\pi$

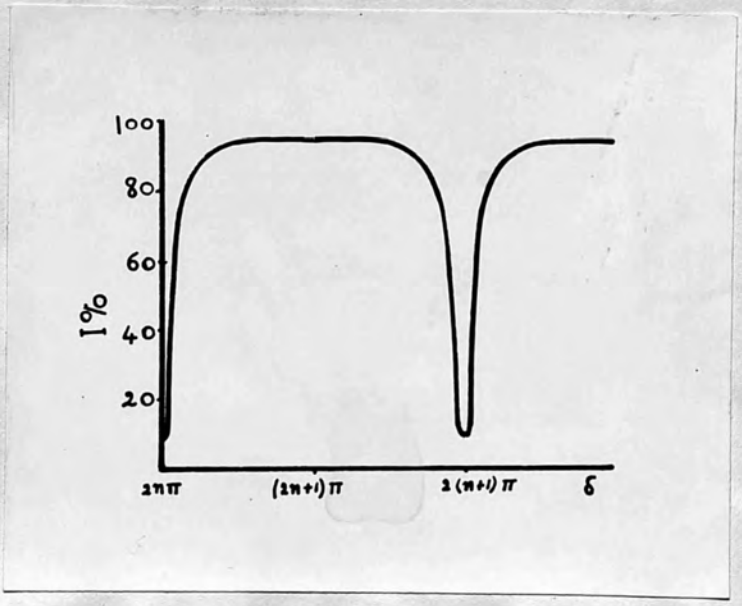

FIG. 6.

The effect of abscrption

$$I_{min} = R\left(1 - \frac{T}{1 - R}\right)^2$$

$$= \frac{R}{(1 - R)^2} A^2 = 0 \text{ for zero absorption.}$$

Therefore the minimum intensity in the reflected system is raised from zero for no absorption to

$$A^2 \frac{R}{(1 - R)^2} .$$

$$I_{max} = R\left(1 + \frac{T^2}{1 + R}\right)^2$$

$$= \frac{R(1 + R + T)^2}{(1 + R)^2} = \frac{R}{(1 + R)^2} (2 - A)^2$$

$$= \frac{4R}{(1 + R)^2} (1 - A)$$

Thus the value of I_{max} obtained in the absence of absorption is decreased by an amount $\frac{4R}{(1 + R)^2} \cdot A$

$$I_{max} \text{ (with absorption)} = I_{max} (A = 0) - \frac{4R}{(1 + R)^2} \cdot A$$

The intensity distribution in the reflected system for R = .85 is shown in Fig. (6)

Fig. (7) shows the contrast as measured by $I_{max} - I_{min}$

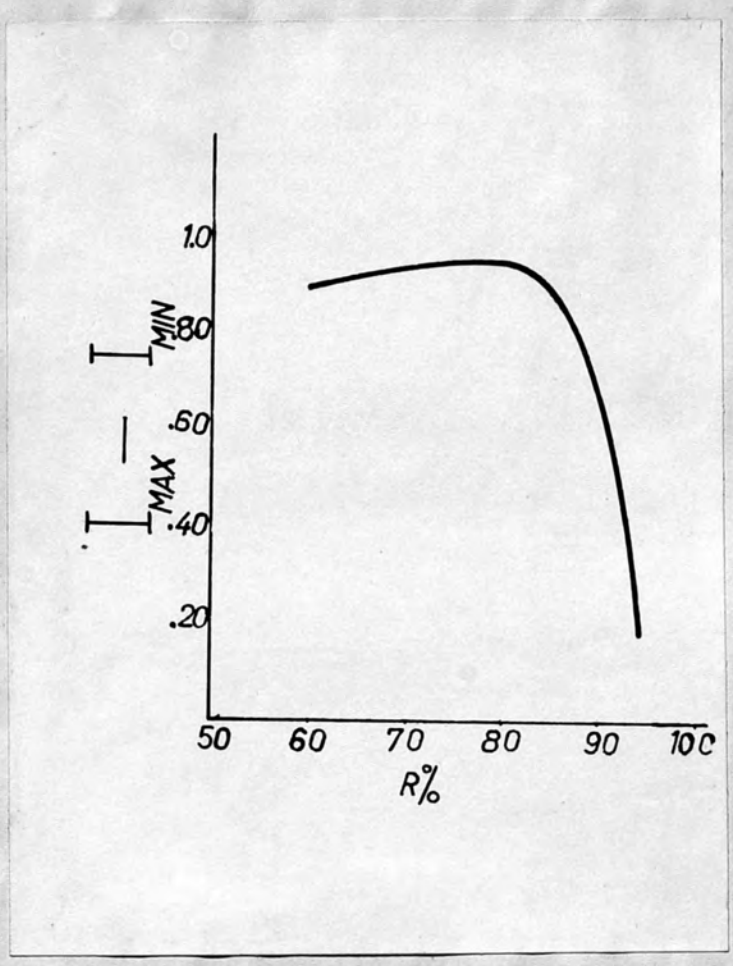

FIG. 7.

Extension to the case of a wedge

It has been shown by Brossel (9) that in the case of a metallically coated air wedge interferometer, the path difference δ_n between the first beam and the n^{th} beam which suffers 2n reflections, for the case of normal incidence, is given to a good approximation by

$$\delta_n = 2\,n\,t\,(1 - \frac{2n^2 + 1}{3}\,\alpha^2)$$

α being the angle of the wedge, t its thickness and n the order of the beam. This equation shows that the intensity distribution on the wedge is not the same as that obtained using a metallically coated plane parallel sheet. The retardation terms when small produce asymmetry in the fringes and as they become greater, secondary maxima occur close to the main maxima. But by choosing a sufficiently small wedge angle and thickness, these terms become negligible and the deductions which were made in the case of a plane parallel sheet then apply. The collimation must be rigorous and a sufficiently large number of multiply reflected emergent beams must be collected. These conclusions were reached earlier by Tolensky (10).

Extension to the case of a lens-plate interferometer

It is evident that the lens-plate interferometer can be regarded as a number of wedges of increasing gap and angle, and provided that the previously mentioned conditions are satisfied, the intensity distribution should be the same as in the case of a plane parallel sheet. Plates I and II show the appearance of the fringes in transmission and reflection respectively for reflectivity in the region of 85%.

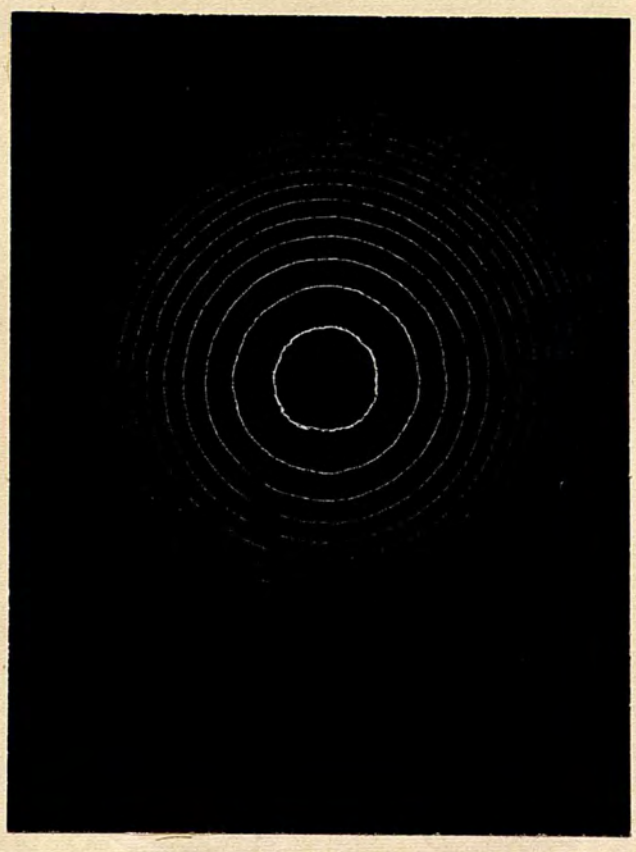

Plate I

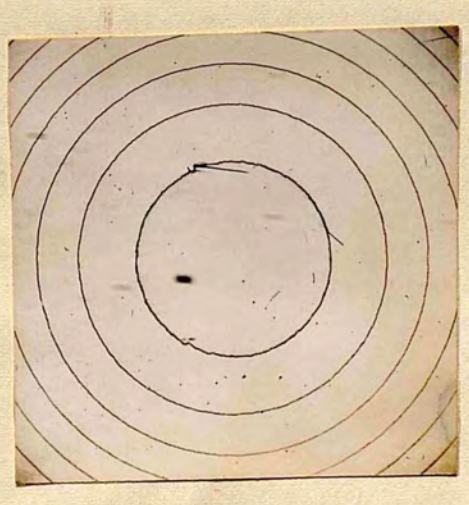

Plate II

CHAPTER II

The relation between the localized monochromatic fringes and the associated white light fringes of equal chromatic order.

The interference taking place when a parallel beam of monochromatic light is incident on a wedge with highly reflecting surfaces has been studied theoretically [11]. In addition to the well known plane of fringe localization close to the wedge, i.e. the Feussner surface of localization[12] whose position is independent of the wavelength used, Brossel [13] (1947) predicted theoretically the presence of an infinite number of other planes of localization at distance x from the Feussner surface given by $x = m \frac{\lambda}{2\alpha^2}$ for the case of normal incidence, α being the angle of the air wedge, λ the wavelength used and m takes the values 1, 2, 3, ... This relation gives the principle Brossel planes only, which are Feussner surfaces of higher order, and is derived by wave fronts or ray tracing. He observed a considerable number of these planes. The dependence of the distance x of such planes of localization on the wavelength is apparent. A variation of $d\lambda$ in λ produces a shift in the plane of localization along the x axis equal to $\frac{x}{\lambda} d\lambda$. Also continuous spectrum between λ and $\lambda + d\lambda$ extends the localization over the same distance dx. Such a distance depends upon the wedge

angle α . Using a white light source, the continuous visible spectrum between 4000 and 8000 A extends the localization over a considerable distance of some centimetres. For $\alpha = 5' 36''$ x = 16.5 cm. for λ = 5461 A and m = 1, and the extension Δ x corresponding to $\Delta\lambda$ = 4000 A is equal to 12 cm.

The formation of fringes of equal chromatic order

Any point on the Feussner surface belongs to a certain t and interference takes place in transmission when the basic condition $n\lambda = 2t \cos\theta$ is satisfied for a certain wavelength λ and order n. The same condition holds for another wavelength λ_1, for $(n + 1)^{th}$ order, ... λ_m for the $(n + m)^{th}$ order. This applies whether the wavelengths are present separately or in a continuous spectrum. Because of the independence of the Feussner surface on the wavelength, these point fringes belonging to different wavelengths are superimposed on each other. They cannot be seen on the Feussner surface, except for very low values of n, as coloured bands starting from the violet to the red

for n = 1 and vanishing due to overlap for higher orders. Now if the Feussner surface is projected on the slit of a spectrograph by an achromat, or the interferometer brought close to the slit, the slit selects a line on the surface, and in general, the thickness t varies along this line. Considering the line to be an infinite number of these point fringes, the dispersive power of the spectrograph separates each set of superimposed points, to be seen on the spectral plane. Let us consider any two points on the line selected by the slit corresponding to t and t + dt. Then for the same order of interference, two point fringes are seen on the spectral plane at wavelengths λ and $\lambda + d\lambda$ where $\frac{t}{\lambda} = \frac{t + dt}{\lambda + d\lambda}$ = Const. n.

If the thickness t changes gradually over dt, a continuous curve for every order of interference results. In the case of a vertical step, t changes abruptly and a discontinuity occurs. The family of white light interference fringes on the spectral plane whose order of interference is constant along every single member, are the fringes of equal chromatic order (Tolansky 1945)[14].

The condition for formation

If the monochromatic localized fringes on any of the principal Brossel planes are projected on a spectrograph slit and white light source is used, the resulting white light fringes seen on the spectral plane are only in focus over a very limited area, depending upon the extension of localization in space as well as the depth of focus of the projecting achromat. We are now in a position to reach the following conclusion: The associated white light fringes of equal chromatic order can only be formed in focus on the spectral plane if the position of the surface of localization of the monochromatic system is independent of the wavelength used. Applying this conclusion to the monochromatic fringes localized on the Fuessner surface of zero order (i.e. $m = 0$), the associated fringes of equal chromatic order obtained on the spectral plane are all in focus.

The shape of the fringes of equal chromatic order

It is clear that the shape of the resulting fringes depends basically upon the way t varies along the line selected by the slit.

If this line is taken to be the y axis, then in general t is a function of y, i.e. $t = f(y)$. The spectral plane is the (λ, y) plane, and thus the shape of fringes of equal chromatic order results directly by transforming the equation $t = f(y)$ from the (t, y) plane to the (λ, y) plane, obeying the relation $n\lambda = 2\mu t \cos\theta$ for the transmitted system, neglecting phase changes at reflection. The shape of the resulting fringes depends basically on the transforming relation. For the reflected system where the relation is $(n + \frac{1}{2})\lambda = 2\mu t \cos\theta$, the narrow dark lines have the same shape as the transmitted fringes. Two factors need to be considered:- (a)m the magnification of the projecting lens and the possible magnification of the spectrograph; (b) the dispersion of the spectrograph. The effect of the magnification due to the projecting lens is only along the direction of the slit, it has no effect along the perpendicular direction - the λ axis - where the dispersive power of the instrument functions. A prism spectrograph or a diffraction grating could be used; in the first case, the dispersion D obeys Hartman's formula

formula[15] $\lambda = \lambda_0 + \frac{B}{D-D_0}$ where λ_0, B and D_0 are constants, while the grating, using the first order, provides a linear dispersion $D = K\lambda$. Confining ourselves to linear dispersion, and substituting for λ and t in terms of D and Y in the basic equation

$$n\lambda = 2\mu t \cos\theta \cdot f\left(\frac{Y}{m}\right)$$

$$D = \frac{2K}{n} \cdot f\left(\frac{Y}{m}\right)$$ for any fringe, at normal incidence using an air medium. This is an equation of a family of fringes of decreasing magnification as n takes the values 1, 2, 3, ... A similar relation has been derived by P. Morris[16]. The above relation shows that any fringe on the (D, Y) plane is a magnified image of the section of the interferometer selected by the slit, and since the effect of the magnification is in general not the same along the D and Y axes, a distorted image is obtained. As an example, elliptic fringes result from a circular section. Using a prism spectograph, another cause of distortion arises which is due to the non-linearity of the dispersion. In particular, this is evident with fringes extending over a considerable range of wavelength, e.g. the bending of straight line fringes resulting from a wedge.

The shape of the fringes of equal chromatic order formed by an air wedge

If α is the angle of the air wedge, one of whose components is adjusted parallel to the plane of the slit, and ϵ the optical separation of the two components at the point of contact, then

$\frac{t - \epsilon}{y} = \tan \alpha$ the equation for the section of the wedge selected by the slit.

$y = \cot \alpha \,.(t - \epsilon)$ a linear function of t.

Substituting in the basic equation, at normal incidence, for interference in transmission on

$n \lambda = 2 t.$

$n \lambda = 2 \tan \alpha \,.y + 2 \epsilon$

$\therefore \quad y = \cot \alpha \,.(\frac{n \lambda}{2} - \epsilon)$

$= \frac{n \cot \alpha}{2} (\lambda - \frac{2 \epsilon}{n})$ (7)

The last equation represents a family of non-parallel straight lines, the slope of each mamber is $\frac{n}{2} \cot \alpha$ where n is an integer. The family has a common point at $(0, - \epsilon \cot \alpha)$ and as n increases the fringes approach the vertical direction of the y axis.

The effect of rotation of the wedge about an axis perpendicular to the plane of the slit on the sloping of the fringes.

The last equation is only valid when the edge of the wedge is perpendicular to the slit, otherwise a resolved component of the true angle of the wedge is obtained. In general if Q is the angle made by the edge of the wedge and the spectrograph slit, then the resolved component β is given by the relation

$$\tan \beta = \tan \alpha \sin Q$$

When the edge of the wedge is parallel to the slit, i.e. $Q = 0$, we have straight line fringes parallel to the slit; this is of course due to the fact that t is constant along the slit. The common point of intersection $(0, -\epsilon \cot \beta)$ goes to infinity. Rotating the wedge as specified, the fringes deviate from parallelism, attaining minimum slope at $Q = \frac{\pi}{2}$, thus giving the true angle of the wedge. Further rotation brings the fringes back again parallel to the Y axis at $Q = 2\pi$.

The case of Newton's rings.

A lens and an optical flat, coated with semi-transparent highly reflecting silver layers, are

brought into contact. The equation of a circle in the (λ, y) plane is

$(t - (R + \epsilon))^2 + y^2 = R^2$ where R is the radius of curvature, and ϵ is the optical separation at the point of contact. The origin is chosen such that at $t = \epsilon$ $y = 0$. Transforming the previous equation to the (λ, y) plane

$$\left(\frac{\lambda - \frac{2(R + \epsilon)}{n}}{\frac{4R^2}{n^2}}\right)^2 + \frac{y^2}{R^2} = 1.$$

This equation represents a family of ellipses whose centres are $(\frac{2(R + \epsilon)}{n}, 0)$ and whose semi major and minor axes are R and $\frac{2R}{n}$, as n takes the positive integer values.

On the (D, Y) plane the equation becomes

$$\frac{\left(D - \frac{2(R + \epsilon)K}{n}\right)^2}{\frac{4R^2K^2}{n^2}} + \frac{Y^2}{m^2 R^2} = 1.$$

which is again an equation of a family of ellipses with centres $(\frac{2(R + \epsilon)K}{n}, 0)$ and whose major and minor axes are m R and $\frac{2RK}{n}$.

Since t is small compared with R, t^2 could be neglected. The resulting equation represents a family of parobolas, as reached by Tolansky[17].

These fringes are convex to the violet as shown in Plate III.

Using a plano-concave lens with its curved surface as one of the components of the interferometer, the equation of the family of the fringes is

$$\frac{\left(\lambda + \frac{2(R - \epsilon)}{n}\right)^2}{\frac{4R^2}{n^2}} + \frac{y^2}{R^2} = 1$$

where ϵ is the sagitta of the curved surface of radius R, with respect to the optical flat. This is an equation of a family of ellipses whose centres are $(\frac{2\epsilon}{n}, 0)$ and which are convex to the red as verified by Plate (IV). Thus for a hill the fringes of equal chromatic order are convex to the violet, while for a valley they are convex to the red. An easy way of relating the concavity of the fringes to the curved surface under investigation is to look for the image of the curved surface in the optical flat.

In deriving the equations representing the shape of the fringes, the variation of the angle of incidence θ is neglected and the condition for interference is taken to be $n\lambda = 2t$ for normal incidence. It is apparent that there is a small variation in θ at the curved surface which is equal to $\sin^{-1} \frac{y}{R}$

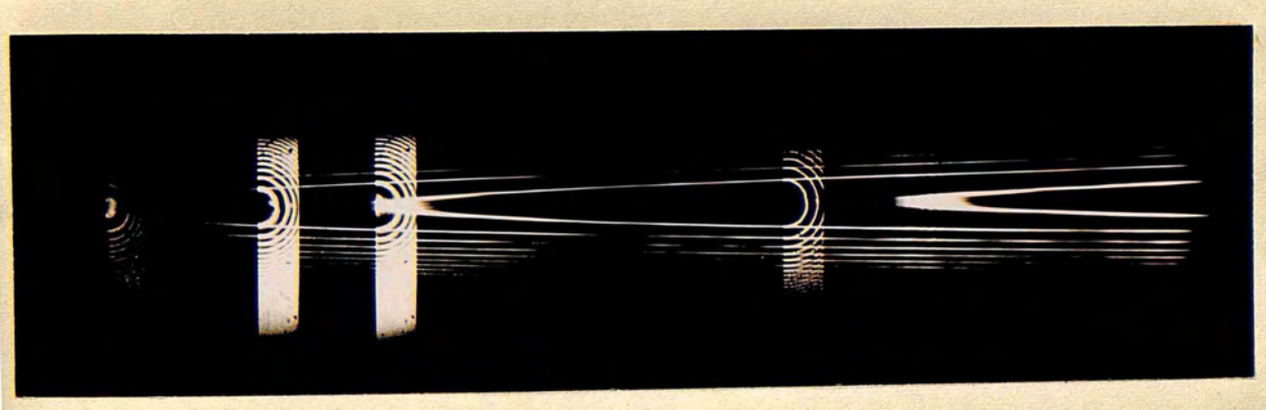

Plate III

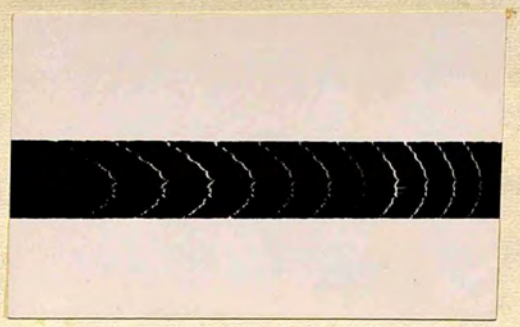

Plate IV

From the previous discussion concerning the formation of fringes of equal chromatic order and their relation to Fizeau fringes, it is clear that all the information obtained from Fizeau fringes along any line on the surface could be obtained more advantageously from the fringes of equal chromatic order. The presence of a family of white light fringes corresponding to a line on the surface in conjunction with the magnification along the axis, enables us to measure the thickness t at any point on the selected line and to remove any ambiguity about concavity.

We can also measure the change of phase at reflection and the variation of the refractive index with wavelength for a dispersive medium. A simple method here suggested for determining the change of phase at reflection is as follows:

For two identically silvered optical flats forming an air wedge, the fringes of equal chromatic order in transmission at normal incidence obey the relation

$$\delta + 2\beta_\lambda = 2n\pi$$

therefore $$2t + \frac{\beta_\lambda}{\pi}.\lambda = n\lambda$$

With the edge of the wedge parallel to the slit, straight lines vertical fringes are obtained. The wave-number difference between any two consecutive fringes of order n and (n + 1) is

$$\Delta v = \gamma_{(n+1)} - \gamma_{v_n} = \frac{\lambda_n - \lambda_{n+1}}{\lambda_n \lambda_{n+1}}$$

$$= \frac{1}{2t} \left\{ 1 - \frac{1}{\pi} \left(\beta_{\lambda_{n+1}} - \beta_{\lambda_n} \right) \right\}$$

As the variation of β_λ with wavelength between two successive orders is small when the fringes are close, the wave-number difference approaches the constant value of $\frac{1}{2}t$. The effective order of interference may be found from the equation

$$n - \frac{\beta}{\pi} = \frac{2t}{n} = \frac{\lambda_{n+1}}{\lambda_n - \lambda_{n+1}}$$

where the fractional part represents β, n being essentially an integer. The last equation leaves us with an ambiguity about the sign and the order of β. A strip of the silvered film on one of the components is removed, the resulting shift in the fringes of equal chromatic order is noted and the apparent thickness of the evaporated silver film is measured (Khamsavi and Donaldson[18] 1947, Avery[19] 1949). Assuming that the phase change at an air/dielectric interface to be an advance of π, the sign and the order of β could be evaluated. Measurements in

the case of air/silver reflection phase change made by a colleague R. Faust[20] showed an advance of $.78\pi$ for $\lambda = 5461$ A$^{\circ}$ $R > 0.7$ which is in agreement with earlier measurements by Rouard[21] 1937.

While Fizeau fringes give a useful contour map of an extended surface area, for surface topography the running of the slit of the spectrograph along a certain line on the contour map is needed. Relating the resulting fringes of equal chromatic order to Fizeau fringes could best be done by the method of superposition.

The Method of Superposition

The fact that the fringes of equal chromatic order and Fizeau fringes can be obtained in focus on the same plate, with the same adjustment, furnishes the basis of the method of superposition. This is done in practice by projecting Fizeau fringes on the slit of a spectrograph which is left wide open. The specimen is adjusted so that the slit when it is narrowed selects the line region under investigation. White light replaces the monochromatic source and the fringes of equal chromatic order are recorded on the photographic plate. The slit is then opened and

the Fizeau fringes are recorded. An interferogram is obtained showing the fringes of equal chromatic order corresponding to the selected line on the surface identified by Fizeau fringes. The direct application is in the measurement of depth or height of any features on the surface, e.g. steps, indentations, abrasions. It is known that in general, Fizeau fringes do not provide enough information for the accurate evaluation of depths of valleys and heights of hills. The associated fringes of equal chromatic order give the true height or depth only if the line selected by the slit passes through the points of maximum height or minimum depth with respect to a line on the surface. Plate (III) shows the appearance of both Fizeau fringes and the fringes of equal chromatic order in the case of a lens-plate interferometer. The spectrograph slit selects a line passing through the centre of the system.

Another important application of the method of superposition is to be seen in the measurement of small surface angles[22]. It has been established[23] that the fringes of equal chromatic order are superior to the Fizeau fringes in the evaluation of

small surface angles, in particular when we are concerned with very small angles extending over small areas. But they suffer from a limitation in that the angle shown by the fringes depends upon the orientation of the surface relative to the spectrograph slit as explained before. A resolved component of any surface angle appears and in general it is necessary to rotate the surface under observation to find the minimum slope corresponding to the true surface angle. This difficulty can be avoided by applying the method of superposition as follows:

Consider a simple wedge between two planes, one vertical, with the edge perpendicular to the spectroscope slit. This leads to the formation of a family of fringes of equal chromatic order given by equation (7). If y_1 is the vertical distance between two fringes, then the wedge angle is $\tan^{-1} \frac{\lambda}{2y_1}$ However, in the general case, the edge of the wedge is not perpendicular to the slit and if Q is the angle made by the edge and the slit, then the true angle of the wedge α is given by the relation $\tan \beta = \tan \alpha \sin Q$ where β is the apparent angle given by the fringes of equal chromatic order, i.e. $\tan \beta = \frac{\lambda}{2y_2}$, y_2 being the vertical distance between two fringes. However, the Fizeau fringes

from a wedge are straight lines parallel to the edge, hence the angle Q is simply the angle made by Fizeau fringes with the slit, i.e. with any spectral line. Clearly a superposition of the two systems enables Q to be measured. This is obtained very easily in practice. The fringes of equal chromatic order are first photographed with the usual source of white light, using a narrow slit. Without moving either the interference system or the photographic plate, the slit is opened wide and the source of white light is replaced by a mercury arc. Fizeau fringes are superimposed on the fringes of equal chromatic order as shown in Plate (V). This is the special case of a wedge set with $Q = \frac{\pi}{2}$, and the Fizeau fringes are horizontal. The Fizeau fringes assist in identifying the intercept of a vertical line with successive fringes of equal chromatic order. In the case shown $\tan \alpha = .000107$ Plates (VI) and (VII) illustrate the appearance when the edge happens to be set with $Q = 60^{\circ}$ and 45°, and it is easy to see how the formula given above enables α to be measured. The agreement between the angles evaluated is seen from table (I). Table II gives the apparent and true angle of another wedge for $Q = 30$ and 60°.

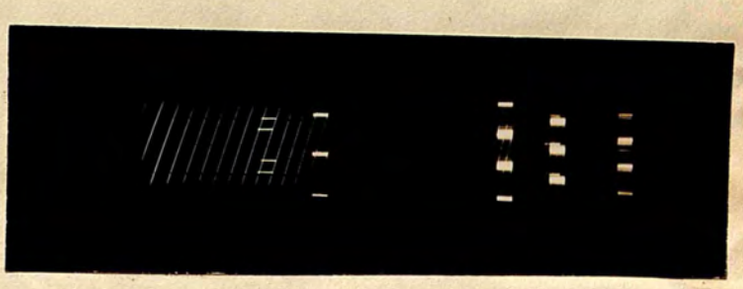

Plate$. (V)

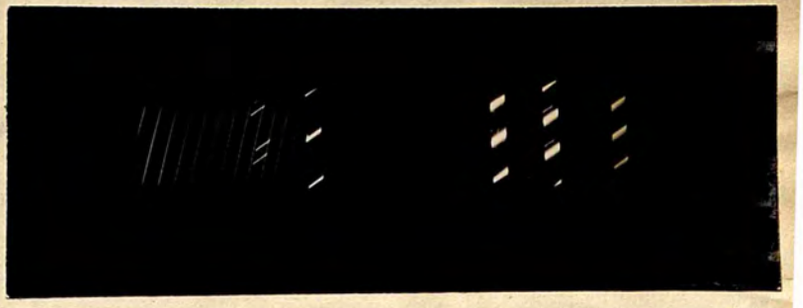

Plate$. (Vl)

Plate$. (VII)

The same method applies using reflection fringes when the surface under investigation is opaque. Because of the unavoidable drop in visibility when any two systems in reflection are superimposed, separate parts of the photographic plate are used. The appearance is as shown in Plate (VIII) $\tan \alpha = .00068$

The previous method was also applied by L. J. Griffin[24] in his important work on growth features of molecular dimensions on crystals. These features do not produce an observed kink when Fizeau fringes run across them. He chose an area in which a large number of these features - edges - suddenly turn through a sharp angle. The true angle was measured and by counting the number of edges and their lateral extension, they were found to be unimolecular steps.

This method is suggested for use in detecting slightly inclined vicinal faces on crystals.

Plate. VIII.

Table I = 5461 A°

Q^{o}	$y_{mm.}$	tan	tan
90	5.10	107×10^{-6}	107×10^{-6}
60	5.90	92.56×10^{-6}	106.9×10^{-6}
45	7.10	76.9×10^{-6}	108.7×10^{-6}

Table II

Q^{o}	$y_{mm.}$	tan	tan
60	6.06	$9. 10^{-4}$	.0001039
30	10.42	5.24×10^{-5}	.0001048

Chapter III

Interferometric studies on cylindrically curved thin films

Section I The theory of formation of the fringes of equal tangential inclination[29]

The only attempt to study the phenomenon of interference in cylindrically curved thin films was made by Raman[25] and Rajagopalan in 1939. They used an extended source of monochromatic light with unsilvered thin sheets of mica in the form of cylinders. The resulting fringes, on transmission and reflection, were broad, non-localized, with shape varying with the observer's position. Their visibility was poor especially in transmission, and no doubling effects due to the birefringence of the mica were observed. These fringes were also obtained with soap bubbles[26].

In this thesis the case of interference taking place when a parallel beam of monochromatic light is incident on an air gap between two high reflecting semi-cylinders with common axis, has been studied. The theoretical treatment is as follows:-

Let S_1 and S_2 represent the line intersections with the XY plane of two reflecting semi-cylinders, of radii of curvature R and R + t respectively. A parallel beam of monochromatic light is incident on S_2 and makes an angle θ with the radius at the point of incidence. It is partially transmitted,

and is incident on the surface S_1 at an angle $(\theta + \beta)$, where β is the angle subtended at the centre by the part of the beam enclosed between the two surfaces. Fig. 8 shows the behaviour of the multiple beams in both transmission and reflection. It is clear that any two successive beams are equally inclined to each other, making an angle 2β, where β is determined by the relation

$$\sin(\theta + \beta) = \frac{R + t}{R} \sin\theta$$

From the geometry of the figure it is seen that the path difference between any two successive beams is the same, i.e. it is independent of the order of the multiple beam. Also all rays which derive from this incident ray and emerge after any number of reflections are tangential to a circle of centre O - the common centre of curvature - with radius equal to $(R + t) \sin\theta$. Hence this circle is the caustic for all rays deriving from the incident ray. These two results hold for both transmitted and reflected systems, the caustic circle being identical for both cases.

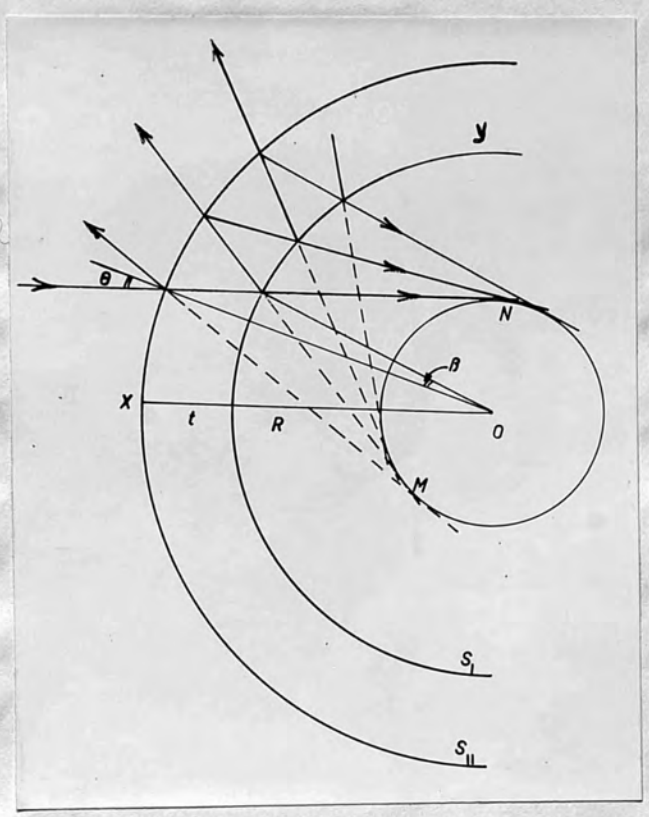

FIG. 8.

If N is the point of intersection of the first and second beams, L that for the second and third and P for the n^{th} and $(n + 1)^{th}$ then PN is the closing side of the polygon of displacements (NL ... P) (see Fig. 8). From geometry, the sides of the polygon (other than PN) are equal and any two successive beams (sides of polygon) make an angle 2β with each other. Resolving the displacements along the direction of the first beam and perpendicular to it and summing the resulting two finite series, expressions for PN_x and PN_y, the components of PN along axes OX and OY, are obtained in the form:

$$PN_x = 2R \frac{\sin(\theta + \beta)}{\cos \beta} \cos n\beta \sin (n - 1)\beta$$

$$PN_y = 2R \frac{\sin(\theta + \beta)}{\cos \beta} \sin n\beta \sin (n - 1)\beta$$

For R = 2 cm., t = 0.01 mm., n = 20 and $\theta = 30^o$ the values of PN_x and PN_y are 0.11 mm. and 0.00064 mm., respectively. It is clear that the distance along the x axis - direction of the first beam - between any two successive points of intersection decreases as n increases, the first displacement MN_x being the largest. For the above numerical example MN_x = 0.0058 mm.

Thus for low order multiple beam interference, in both transmission and reflection, the beams could be considered to intersect at practically the same point N for the transmitted system and M for the reflected system. The coordinates of N with respect to the two rectangular axes OX and OY are

$$x = R \frac{\cos \theta}{\cos \beta} - R \cos (\theta + \beta)$$

$$y = R \sin (\theta + \beta)$$

These equations give the locus of the point N as the angle of incidence θ varies according to the relation $-\frac{\pi}{2} \leq (\theta + \beta) \leq \frac{\pi}{2}$. As θ tends to zero, β tends also to zero and consequently both X and Y vanish. Therefore the locus of the point N passes through the origin O at $\theta = 0$, and as θ increases it begins to deviate slowly from OY. The deviation x increases rapidly for higher angles of incidence towards the limiting value $(2 R t + t^2)^{\frac{1}{2}}$ for $Y = R$ and $\theta = \sin^{-1} \frac{R}{R + t}$. For R = 2 cm. and t = 0.01 mm., the limiting value of x is 0.6 mm., when θ is very nearly equal to $\frac{\pi}{2}$. Therefore for values of t/R of the order of 1/1000 the locus of the point N could be considered to be approximately a straight line coinciding with OY.

The coordinates of the point M with respect to the same axes are

$$x = -\left\{(R + t)\cos\theta - (R + t)\frac{\cos(\theta + \beta)}{\cos\beta}\cos 2\theta\right\}$$

$$y = \left\{(R + t)\sin\theta - (R + t)\frac{\cos(\theta + \beta)}{\cos\beta}\sin 2\theta\right\}$$

Fig. 9 shows the locus of M as the angle of incidence varies for the case of R = 2 cm. and t = 0.01 mm. The path difference between any two successive beams

$$= R\frac{\sin\beta}{\sin\theta}\cdot\frac{\sin 2(\theta + \beta)}{\sin 2\beta} + R\frac{\sin\beta}{\sin\theta} - R\frac{\cos\theta}{\cos\beta}$$

$$= 2t\cos\theta\left(1 - \sin\beta/2\,\frac{\sin\theta}{\cos(\theta + \beta/2)\cos\beta}\right)$$

$= 2t\cos\theta\,(1 - \frac{1}{2}\beta\tan\theta)$ neglecting terms involving β^2 and higher powers

$$= 2t\cos\theta - \Delta_\theta t \quad \text{where } \Delta_\theta = \beta\sin\theta \qquad (8)$$

The shape of the fringes

From the previous discussion the fringes are of equal θ, i.e. the tangential inclination is constant along each fringe. In the case of two semi-cylinders with common axis, the fringes are straight lines parallel to the generator, while for two concentric hemispheres the fringes are concentric circles. It is proposed to call these fringes "fringes of equal tangential inclination". (27)

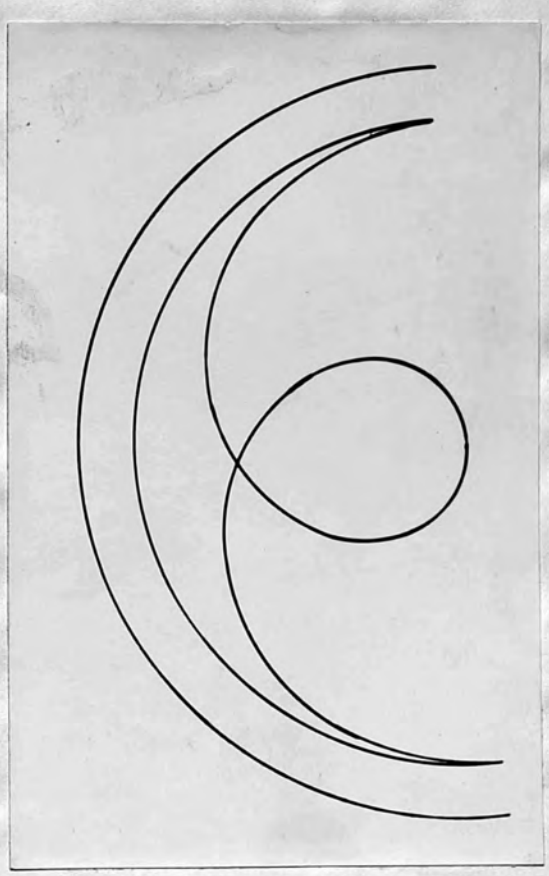

FIG. 9.

Their relationship to the fringes of equal inclination is clear, for as R increases, the localized fringes move away from the interferometer and become identical with fringes of equal inclination[28] when R becomes infinite, i.e. when S_1 and S_{11} are plane parallel.

Localization of fringes

Both transmitted and reflected systems are not formed on planes but on surfaces of localization. A point of importance is the continuity of these surfaces at the centre where θ is equal to zero.

In the case of the transmitted system a considerable number of fringes are in focus on a photographic plate placed at O normal to OX. The interferometer is behaving in a sense as a lens, similar to a non-parallel sided Lummer plate[29]. The focal length is equal to the radius of curvature R, with focal defects at high angles of incidence. A projecting lens could minimise these defects.

In the case of the reflected system, only a very limited number of fringes could be brought to focus at a time.

The focal properties of the interferometer depend upon whether the concavity is towards or away from the source. In the case shown in Fig. 8 the transmitted system is real while the reflected system is virtual. The reflected system is on the other side of the interferometer away from the source. The opposite takes place when the interferometer is rotated through 180 degrees.

The number of interfering beams

It is clear that the number of interfering beams is finite, since they terminate at the end of the interferometer, whose length decreases as θ increases for the case shown in Fig. 8. For a certain R and t, the curvilinear displacement of the multiple reflected beams increases with θ. It is equal to $2 R\beta$. Thus for the case mentioned above, the number of interfering beams decreases as the angle of incidence increases. The variation of the reflectivity of the surface S_1 and S_2 with θ only affects the distribution of the incident intensity among the beams. For the case of R = 2 cm., t = .01 mm. and $\theta = 30^{\circ}$, a length of arc equal to .34 mm. is needed for producing 30 beams.

Departure from parallelism

Let A be the point of incidence of a ray whose angle of incidence is θ. Now if the incident ray is exactly parallel to the axis, the height of incidence Y is equal to $(R + t) \sin \theta$, and the resulting fringe is localized on a plane through O perpendicular to the direction of the incident ray - represented by ON in Fig. 10. Let OA be the radius through the point of incidence. A deviation from parellelism, towards or away from OA, brings N to N_1 and N_{11} respectively. Therefore the surface of localization is curved - for divergent incident beams, towards the bent film and for convergent beams, away from the film as shown in Fig. 10.

A further point of importance is to be seen in that the caustic circle is the same for all wave-lengths. Therefore, the condition for the formation of the associated system of white light fringes of equal chromatic order, as mentioned on page 20 is satisfied.

The associated system of white light fringes

If a source of white light is used in place of the monochromatic source and the transmitted system is projected on the slit of the spectrograph,

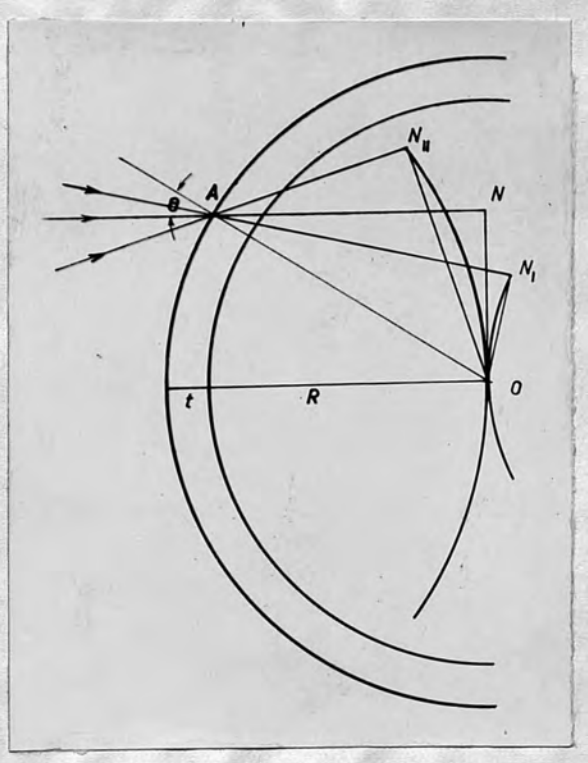

FIG. 10.

fringes of equal chromatic order are seen. They are localized fringes of constant $\frac{\cos\theta}{\lambda}$, neglecting Δ_θ in equation (8). The general shape of these fringes when the common axis of the interferometer is perpendicular to the plane of the slit is derived as follows:-

Considering the condition of interference in transmission to be $n\lambda = 2t\cos\theta$ and since $\sin\theta = \frac{y}{R+t}$ then we have

$$n^2\lambda^2 = 4t^2(1 - \sin^2\theta)$$

$$n^2\lambda^2 = 4t^2\left(1 - \frac{y^2}{(R+t)^2}\right)$$

$$\frac{n^2\lambda^2}{4t^2} + \frac{y^2}{(R+t)^2} = 1$$

Thus the shape of the fringes is given by the equation

$$\frac{\lambda^2}{\frac{4t^2}{n^2}} + \frac{y^2}{(R+t)^2} = 1$$ where n takes successive integral values.

This equation represents, on the spectral plane (λ, y), a family of ellipses whose major and minor axes are $(R+t)$ and $\frac{2t}{n}$ respectively. At the centre of the system $y = 0$ and $\gamma = \frac{n}{2t}$, therefore the wave number separation between any two consecutive fringes is equal to $\frac{1}{2t}$.

As the interferometer is rotated through $\frac{\pi}{2}$, its generator becoming parallel to the slit, straight line fringes of equal wave number separation are obtained. There is no variation of the angle of incidence θ along these fringes. Their equation on the spectral plane is $\lambda = \frac{2\,t\cos\theta}{n}$ where n takes successive integral values.

Section II

The fringes of equal tangential inclination formed by an interferometer enclosing a refracting medium

Let S_1 and S_2 represent the intersections with the XY plane of two highly reflecting semi-cylinders of radii of curvature R and R + t respectively, enclosing a medium of refractive index . A parallel beam of monochromatic light incident on the interferometer and making an angle θ with the radius at the point of incidence, suffers multiple reflections as shown in Fig. 11. From geometry we have

$$\frac{A\beta}{\sin\beta} = \frac{R}{\sin\gamma} = \frac{R+t}{\sin(\gamma+\beta)}$$

From triangles BGO and BGN

$$BG = 2R\sin\beta$$

and $$\frac{BG}{\sin 2\beta} = \frac{BN}{\sin\left(\epsilon + \frac{\pi}{2} - \beta\right)} = \frac{GN}{\sin\left(\frac{\pi}{2} - \beta - \epsilon\right)}$$

Therefore

$$BN = 2R\frac{\sin}{\sin}\cos(\epsilon - \beta) = R\frac{\cos(\epsilon-\beta)}{\cos\beta}$$

and the coordinates of the point N with respect to OX and OY are

$$x = R\frac{\cos(\epsilon-\beta)}{\cos\beta}\cos(\epsilon - (\theta+\beta) - R\cos(\theta+\beta) \quad (9)$$

$$y = R\sin(\theta+\beta) + R\frac{\cos(\epsilon-\beta)}{\cos\beta}\sin(\epsilon-(\theta+\beta)) \quad (10)$$

$$\frac{R}{\sin\gamma} = \frac{R+t}{\sin(\gamma+\beta)} \quad \text{and} \quad \frac{\sin\theta}{\sin} = \mu = \frac{\sin\epsilon}{\sin(\gamma+\beta)}$$

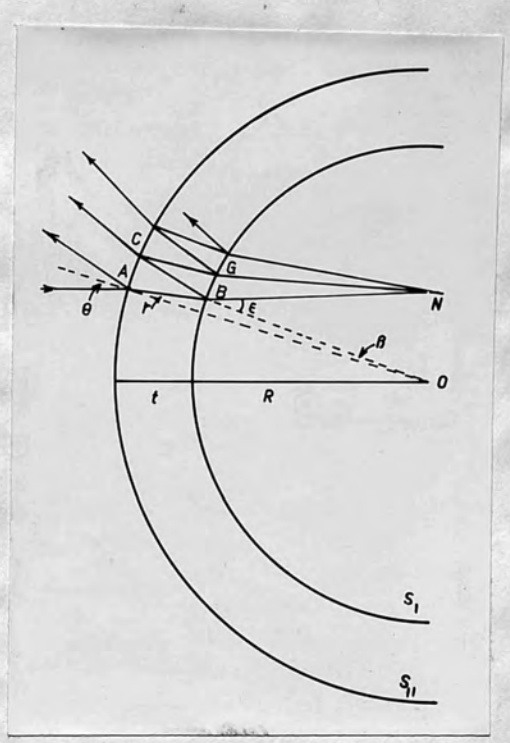

FIG. 11.

The path difference between any two successive beams

is equal to GN + 2μMCB - BN

$$= 2\mu R \frac{\sin\beta}{\sin\gamma} - \frac{R}{\cos\beta}(\cos(\epsilon-\beta) - \cos(\epsilon+\beta))$$

$$= 2\mu t \cos\gamma \left\{ 1 - \sin\beta/2 \frac{\sin\gamma}{\cos(\gamma+\beta/2)\cos\beta} \right\} \quad (11)$$

$$= 2\mu t \cos(\gamma+\beta) \left\{ 1 - \sin\beta/2 \frac{\sin(\gamma+\beta)}{\cos(\gamma+\beta/2)\cos\beta} \right\}$$

Muscovite mica as an isotropic medium

It is known that by using polarised light, it is possible to make a biaxial crystal act as if it were isotropic[30]. Fig. 12 represents an eighth of the wave surface of an optically negative biaxial crystal such as muscovite. The X, Y and Z axes denote the principal vibration directions in the crystal. The X axis represents the vibration-direction of maximum velocity v_g and minimum refractive index μ_p, Y axis for the medium velocity and refractive index v_m and m, and the Z axis for the minimum velocity v_p and the maximum refractive index μ_g. For muscovite mica, the X axis is the acute bisectrix of the optic axial angle and the optic axial plane is very nearly perpendicular to the cleavage plane Zy[31]. Circular sections of the wave front are indicated by continuous lines and the

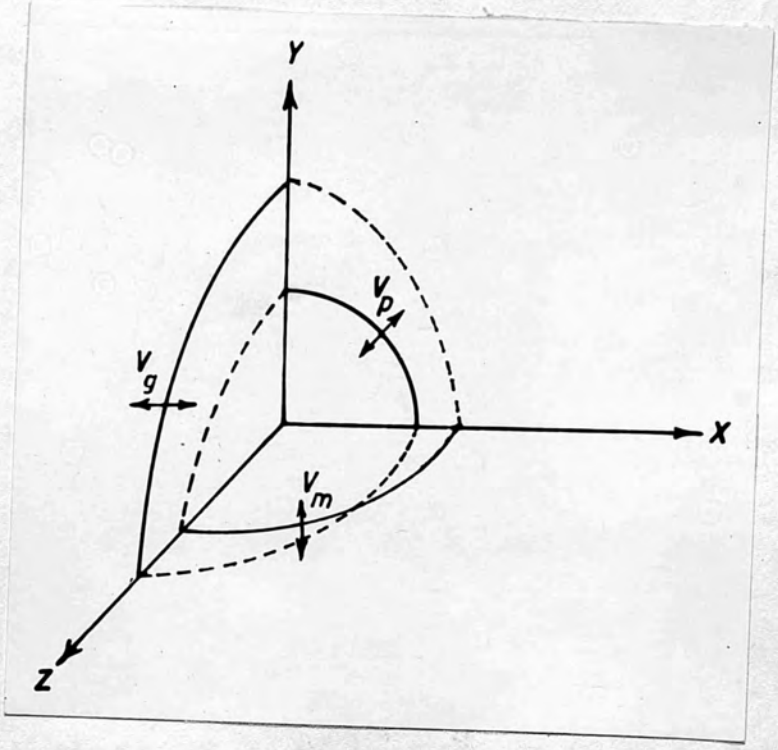

FIG. 12.

arrows show the direction of the electric vector in the wave. The condition for constant refractive index is satisfied by having the common plane of incidence and polorisation either the plane containing the optic axes or the plane at right angles to it. In other words, if the plane of incidence is the optical axial plane, then for light vibrating perpendicular to the plane of incidence, the electric vector parallel to the surface will have a constant refractive index μ_m. If the plane of incidence is at right angles to the optical axial plane then light vibrating perpendicular to the plane of incidence will have a constant refractive index μ_g.

Another reason for using muscovite mica is that it exhibits cleavage in a highly developed form. These sheets could easily be obtained and they are flexible.

Arrangement of apparatus

A piece of high quality muscovite mica was selected, the plane containing the optic axes determined by means of the polarising microscope. A thin film of cross-section some 3 x 4 cm. and thickness about 0.02 mm. was cleaved parallel to

(001) and doubly silvered. The silver deposited possess the usual high reflecting coefficient employed in multiple-beam investigations[32], care being taken to note the position of the optic axes relative to the thin film. The film was then bent in the form of a cylinder of known radius of curvature, suitable radii of curvature are 1 - 5 cm. The direction of bending was the intersection of the optical axial plane with the cleaved surfaces. It was mounted in a special jig - shown in Fig. 13 - so that the plane of incidence coincides with the optical axial plane. Fig 13b represents one of the two identical brass plates used for the jig. The thick semicircles are groves of radii of curvature from half a centimetre up to seven cm. The two plates are fixed to four pillars by screws. The axis of the specimen, bent in the form of a cylinder, can be rendered vertical or horizontal by the two perpendicular stands shown in Fig. 13a.

A parallel beam of monochromatic light was incident on the curved film (Fig. 14) and a nicol prism was inserted between the source and the interferometer. The plane of incidence, which is the optical axial plane is in the plane of the paper.

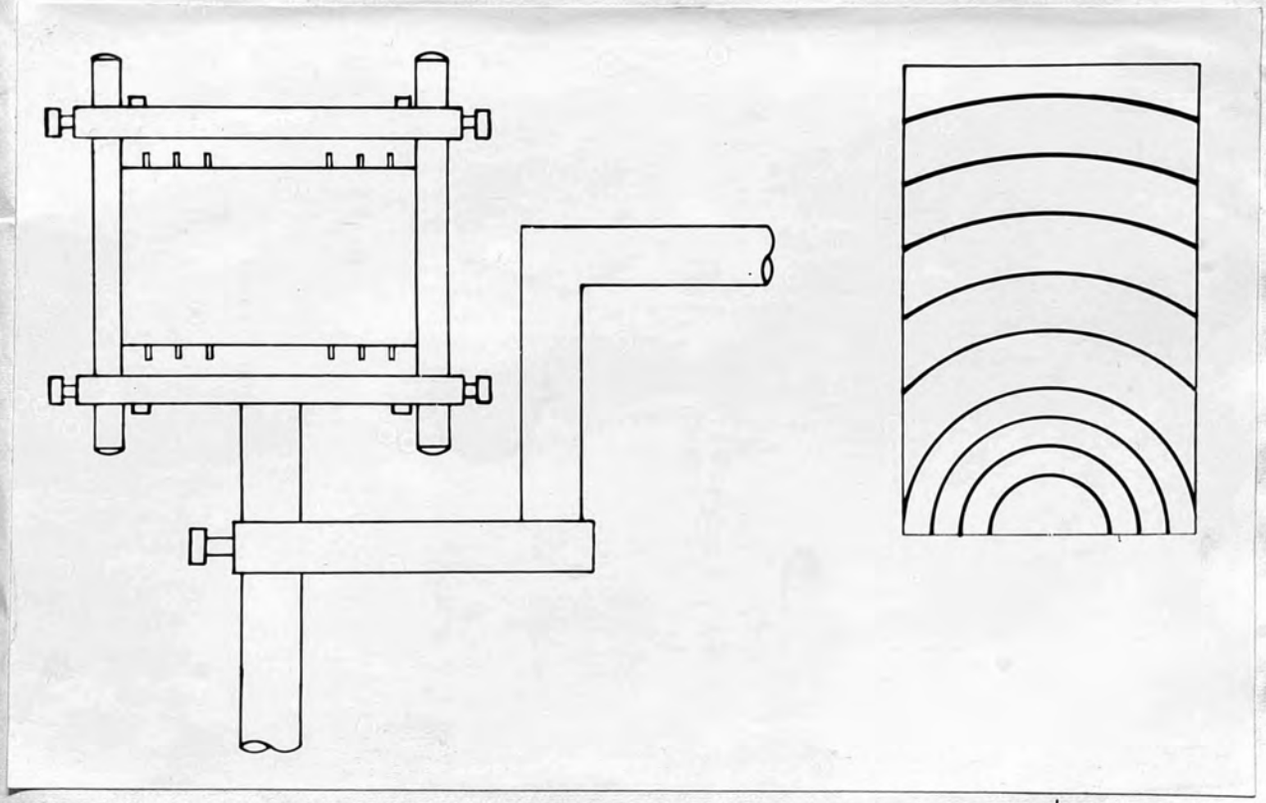

a b

FIG. 13.

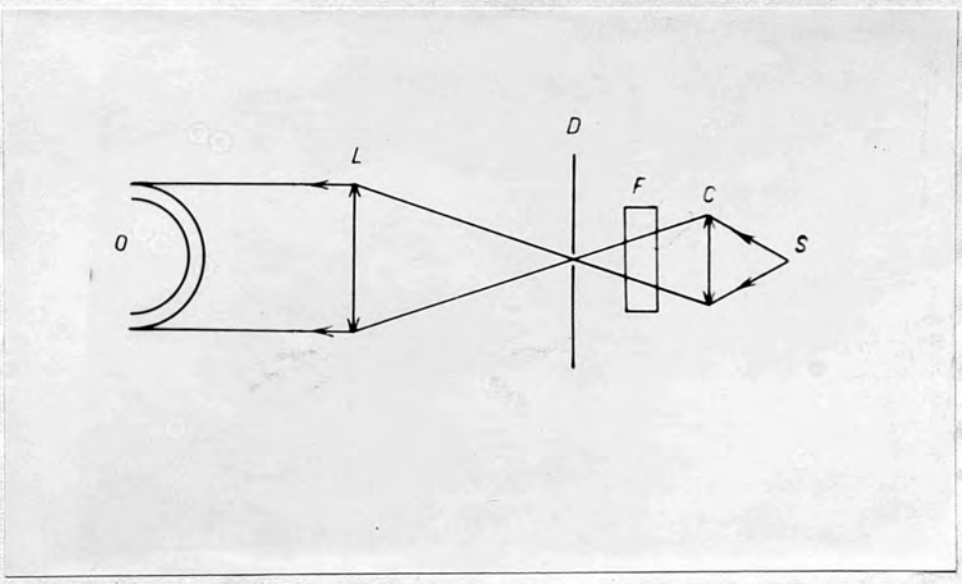

FIG. 14.

The transmitted light vibrated parallel to the shorter diagonal of the prism and was thus perpendicular to the plane of incidence. A system of straight line localised fringes parallel to the axis of the cylinder appeared on a screen placed at O - Plate (IX).

Localization of the fringes of the transmitted system

The resulting fringes were very sharp, and critically localised on a surface which was very nearly plane, for angles of incidence less than $\pi/3$. This surface of localization is given by equations (9) and (10). The radius of curvature of the cylinder was varied and the following table gives the observed and calculated values of the distance D between the surface of the cylinder and the plane of localization.

$t = 0.02$ mm. $\theta = 30^{\circ}$ $\lambda = 5890$ A
$\mu = 1.59$ (By Becke line[33])

R	D calculated	D observed
1.5	1.30	1.32
2	1.73	1.68
3	2.60	2.60
4	3.46	3.40
5	4.33	4.20

All the figures are in cm. For greater values of the radius of curvature R, the fringes became broadened and it was difficult to locate their position with the same degree of accuracy.

Condition for interference

From equation (11) the condition for interference is

$$n\lambda = 2\mu t \cos\gamma \left\{1 - \sin\beta/2 \frac{\sin\gamma}{\cos\beta \cos(\gamma + \beta/2)}\right\}$$

$$= 2\mu t \cos\gamma - 2 u t \sin\beta/2 \frac{\sin\gamma\cos\gamma}{\cos\beta\cos(\gamma + \beta/2)}$$

$$= 2\mu t \cos\gamma - \Delta_\gamma . \mu t$$

This deviation $\Delta = \Delta_\gamma . \mu t$ from the basic law of interference increases as θ increases and is equal to zero at normal incidence. For low order multiple-beam interference, which is the case studied here, the value of the deviation Δ for $\theta < \frac{\pi}{3}$ is much smaller than the change of phase at reflection mica/silver for high reflectivities[34].

e.g. For t = 0.02 mm., R = 2 cm., $\theta = \frac{\pi}{3}$ and $\mu = 1.59$ $\Delta = 96$ A°.

The order of interference increases inversely as the distance from the centre. This is clear from the relation $n = n_0 \cos\gamma$, where n_0 is the

order of interference at the centre of the system and n the corresponding order at a refracting angle r.

The fringe separation law for successive orders

At the centre of the system the order of interference, n_o, is a maximum, given by $n_o \lambda = 2\mu t$. Consider a symmetrical system with fringes on either side of the axis OX. Let the distance between a pair of symmetrically situated fringes on either side of this axis be called $2S$, the diameter of the fringes. If n is the order of interference for the pth fringe, counting from the centre outwards, then by analogy from the well-known corresponding Fabry-Perot theory[35], one obtains the following equation for the fringe separation.

Let r be the angle of refraction within the film, then as $n_o = \frac{2\mu t}{\lambda}$, the order n for the refracting angle r is $n = n_o \cos r$ giving

$$n = n_o \left[1 - \sin^2 r\right]^{\frac{1}{2}}$$

$$= n_o \left[1 - \frac{\sin^2 \theta}{2}\right]^{\frac{1}{2}}$$

If S_p denotes the linear radius of the p th ring,

$$\sin \theta = \frac{S_p}{(R + t)} \text{ to a close approximation}$$

and

$$\frac{n}{n_o} = \left[1 - \frac{S_p^2}{\mu^2 (R + t)^2}\right]^{\frac{1}{2}}$$

In general the order of interference n_o at the centre is non-integral, i.e. $n_o = n_1 + \epsilon$, where ϵ is a fraction and n_1 the order of the first fringe. The order of the p th fringe is given by $n = n_o - (P + \epsilon - 1)$

Hence $(1 - \frac{P + \epsilon - 1}{n_o})^2 = 1 - \frac{S_p^2}{\mu^2 (R + t)^2}$

As p is small compared with n_o then

$$\frac{2}{n_o} (P + \epsilon - 1) = \frac{S_p^2}{\mu^2 (R + t)^2} \quad \text{approximately}$$

giving

$$S_p = \mu (R + t) \sqrt{\frac{2}{n_o} (P + \epsilon - 1)}$$

$$S_p = (R + t) \sqrt{\frac{\mu\lambda}{t} (P + \epsilon - 1)}$$

The scale of the fringe pattern is therfore directly proportional to R and inversely proportional to $t^{\frac{1}{2}}$. Plates (IX) and (X) illustrate the fringes given by a piece of muscovite mica acting as an isotropic medium, in which R has the respective values of 1.5 and 2 cm. By assuming for simplicity that n_o is integral, i.e. $\epsilon = 0$ the scale of the pattern can be readily calculated. Thus for R = 5 cm. and t = 0.02 mm. the diameter of the fringe for λ = 5461 A is very nearly 4 cm.

Thus the fringes are easily seen with the naked eye if they fall on a ground glass screen placed in the plane of localization.

Table

	R	S_1	S_2	S_3	S_4	S_5
A	2	1.79	2.55	3.15	3.70	4.15
B	1.5	1.32	1.88	2.30	2.68	2.98
A/B	1.33	1.36	1.36	1.37	1.38	1.39

Cleavage effects : measurement of steps.

If the selected mica exhibits cleavage steps the result is the production of fringes as shown in Plate (XI) in which the cleavage discontinuities are evident. Let t be the thickness of the mica in a region where a cleavage step takes place and dt is the increment due to the step. Then near the centre of the system $dt = \frac{\lambda}{2\mu} . dn$, where dn is the fractional change of order produced by the step dt at a certain angle of incidence. With monochromatic light the direction of displacement and any intergers of fringe overlapping cannot always be easily decided. In special cases where there is perfect or imperfect coincidence between two fringes at a discontinuity, as in the regions A, B,

C and D in plate (XI), the direction of steps can be deduced from the corresponding fringe separation. It is clear that $t_A > t_B > t_C > t_D$. But if several distinct wavelengths are used, the direction and exact number of orders can both be determined[36].

It is clear that the fringes offer a new precision method for the measurement of cleavage steps, because a change of one order requires a change of thickness of $\frac{\lambda}{2\mu\cos r}$, i.e. 1700 A near the centre in the green. Since the fringe sharpness permits the detection of one-hundredth of an order displacement, then steps of 17 A can be detected.

This property does not depend on the absolute value of t except in so far as the latter affects the whole scale. This is a marked advantage over the fringes of equal chromatic order.

Particularly valuable features in this connection are (a) the high fringe dispersion available without any auxiliary equipment, (b) the flexibility in dispersion which can be controlled by varying the radius of curvature R. The latter can be adapted to the value of t.

The intensity distribution in the transmitted system

The factors affecting the distribution of intensity are (a) the reflectivity and absorption of the deposited silver layers and their mode of variation with the angle of incidence θ, (b) the absorption of the refracting medium, whose effect increases with the optical path of the beam, i.e. with increasing θ, (c) the effect of the increase in the displacement of the multiply reflected beams with θ which effectively reduces the number of interfering beams.

The last factor (c) is a minor one for angles of incidence less than $\frac{\pi}{3}$, since only 1.36 mm. are required to produce 60 beams for $t = 0.02$ mm., $R = 2$ cm. and $\theta = 60^{\circ}$.

Fig. 15 shows a microphotometric trace for the transmitted fringes. The intensity distribution for each fringe is similar to the Fabry-Perot distribution. Both the peak intensity and the half-width of the fringes decrease with n. This is due to the effect of the increasing absorption in the interferometer and reflectivity of the silver layers as θ increases.

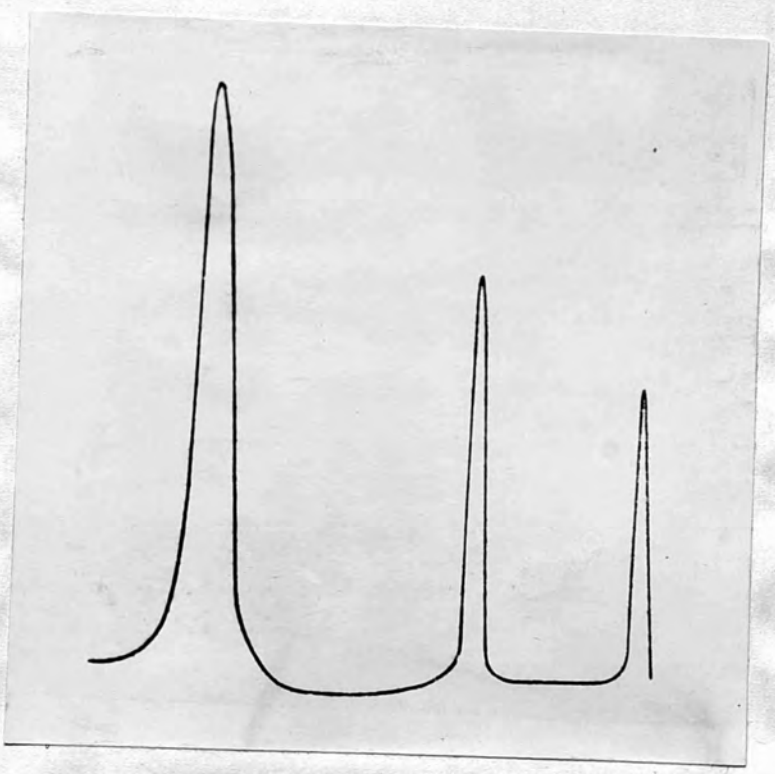

FIG. 15.

The reflected system

The arrangement shown in Fig. 14 produces a real transmitted system while the reflected fringes are virtual and arise from diverging beams. As the interferometer is rotated through 180 degrees, a real reflected system is produced and can be seen on a ground glass screen placed near the interferometer but to one side of the path of the incident light. Only a few fringes could be brought into focus at one time because of the nature of the surface of localization discussed before. Plate (XII) shows the reflected system of fringes, which are narrow dark straight lines on a bright background. Plate (XIII) shows the reflected system produced by an unsilvered piece of mica. The fringes are reasonably sharp owing to the high Fresnel reflecting co-efficients of the uncoated mica arising from the high angles involved.

The associated transmitted white light fringes

With the arrangement shown in Fig. 14 the transmitted system was projected on to the slit of a spectrograph and white light was used in place of the monochromatic source. The associated system of constant $\frac{\cos\theta}{\lambda}$ was seen in focus in the spectral

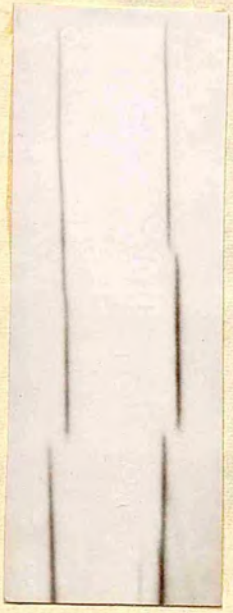

Plate. XII.

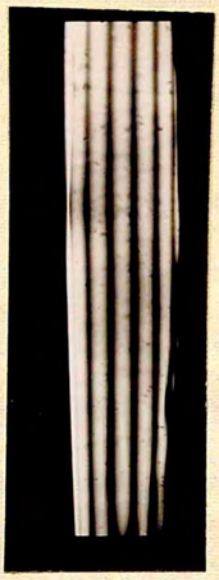

Plate. XIII.

plane. Plate (XIX) shows the transmitted system with mica as the refracting medium. The shape of the fringes is given by

$$\frac{n^2 \lambda^2}{\frac{4\mu^2 t^2}{n^2}} + \frac{S^2}{\mu^2 (R + t)^2} = 1$$

This equation represents a family of fringes in the (λ, S) plane. Along any fringe θ and λ (and consequently μ) vary, but considering the variation of μ to be small, especially when the fringe extends over a small range of wavelength, the last equation gives the shape of the system over that range of wavelength. Assuming the linearity of the dispersion of the spectrograph, the equation represents a family of ellipses with major axis $\mu(R + t)$ and minor axis $\frac{2t}{n}$. As R increases the curvature of the fringes decreases. At normal incidence S = 0 and $\lambda = \frac{2\mu t}{n}$. The coordinates of any point on a fringe is given by $(\frac{2\mu t}{n} \cos\gamma , \mu(R + t) \sin\gamma)$. A spectral line superimposed on the fringes assists in determining the values of at the points of intersection. Taking into account both the magnification of the projecting lens and the possible magnification of the spectograph, θ can be determined to a fair degree of

Plate. XIV.

accuracy even if only an approximately value of t is known.

Section III

Application of the fringes of equal tangential inclination to isotropic media

Magnesium fluoride was chosen as the isotropic medium (37). A thin sheet of freshly cleaved mica, free from inclusions was used as a substrate, and thin films of silver, MgF_2 and silver were successively evaporated on to it. The reflectivity of the silver layers was about 90%. The same optical arrangement for white light fringes as described before was used. The appearance of the fringes is as shown in plate (XV). The plate shows that

(a) as the angle of incidence increases, the fringe is split into two perpendicularly polarised components, the inner component vibrating perpendicular to the plane of incidence.

(b) the components are of different intensities and width, due to the differential absorption and reflectivity of the layers of the interferometer.

The doubling of the fringe arises from the phase change at reflection at a metallic surface -

Plate. XV.

Tolansky 1945(38) - which for non-normal incidence is different for the two polarised components.

Thus the two smooth curves traced by the light itself show the behaviour of the differential change of phase at reflection - MgF_2/ Ag - with the angle of incidence.

The change of phase at reflection at a certain surface is a function of θ, λ and η, where θ is the angle of incidence, the wavelength of the incident light and η the azimuth of the plane of polarisation. In the case of air/Ag/MgF_2/Ag/mica, r is the angle at which the light reaches the silver layers from the magnesium fluoride film.

The condition of interference is therfore

$$n\lambda = 2\mu t \cos r + 2f(r, \lambda, \eta) \qquad (12)$$

If the change of phase is in an advance, the value of the function $f(r, \lambda, \eta)$ is a negative quantity; and is positive for a retardation, which effectively increases the path difference between the multiple beams, i.e. the separation between the two components of the interferometer. The differential change of phase is $[f^{\perp} - f^{\parallel}]_{r,\lambda=const}$ as measured in units of path difference, and is $\left[\frac{f^{\perp} - f^{\parallel}}{\lambda}\right]_{r,\lambda=const.}$ as a fraction of the

wavelength used. Thus for normal incidence the differential change of phase is zero, since there is no distinction between directions parallel and penpendicular to the plane of incidence.

The general shape of the fringe is (as previously proved) part of an ellipse and very nearly a parabola as shown in Plate (XV).

The Determination of the Differential Change of Phase at Reflection MgF_2/Ag.

The conditions of interference for the two mutually polarised components at right angles are

$$\eta\lambda = 2\mu t\cos r + 2f(r,\lambda,n_\perp)$$

and $\eta(\lambda+d\lambda) = 2\mu t\cos r + 2f(r,\lambda+d\lambda,n_{\parallel})$ for the same angle and assuming u to be constant over the range of wavelength $\lambda \longrightarrow \lambda+d\lambda$

Hence $\eta\frac{d\lambda}{2} = f(\lambda,n_\perp) - f(\lambda+d\lambda,n_{\parallel})$

at $r=r_1$ $\eta\frac{d\lambda}{2} = f^{\perp}(\lambda+\frac{d\lambda}{2}) - f^{\parallel}(\lambda+\frac{d\lambda}{2})$ (13) approximately for small $d\lambda$ and at $r=r_1$. The last equation gives the differential change of phase $[f^{\perp}-f^{\parallel}]_{\lambda+\frac{d\lambda}{2},r=r_1}$ in terms of the order of interference and the horizontal separation $d\lambda$. It is clear that the lower the order η, the higher the value of the horizontal separation $d\lambda$ of the two components.

In our case the order is very low, so that we cannot assume that $d\lambda$ is small compared with λ . Consequently the previous equation will only give an approximate estimate of the differential change of phase.

Evaluation of the order of interference

When the optical thickness of the interferometer is plotted against the wavelength for n = 1, 2, 3, ... a family of straight lines of slope which decreases as n increases are obtained (Donaldson) (39). The number of fringes present over a certain range of wavelength is given by the points of intersection of the vertical line indicating the optical thickness of the interferometer with the sloping lines. The presence of one fringe in the field of view between 4000 - 8000 A indicates that its order is either one or two (40).

A similar diagram between $n\lambda$ and λ can be used to show the behaviour of the fringes as the angle of incidence increases, and ultimately the order of the fringe can be determined if only one fringe is present Fig. (16).

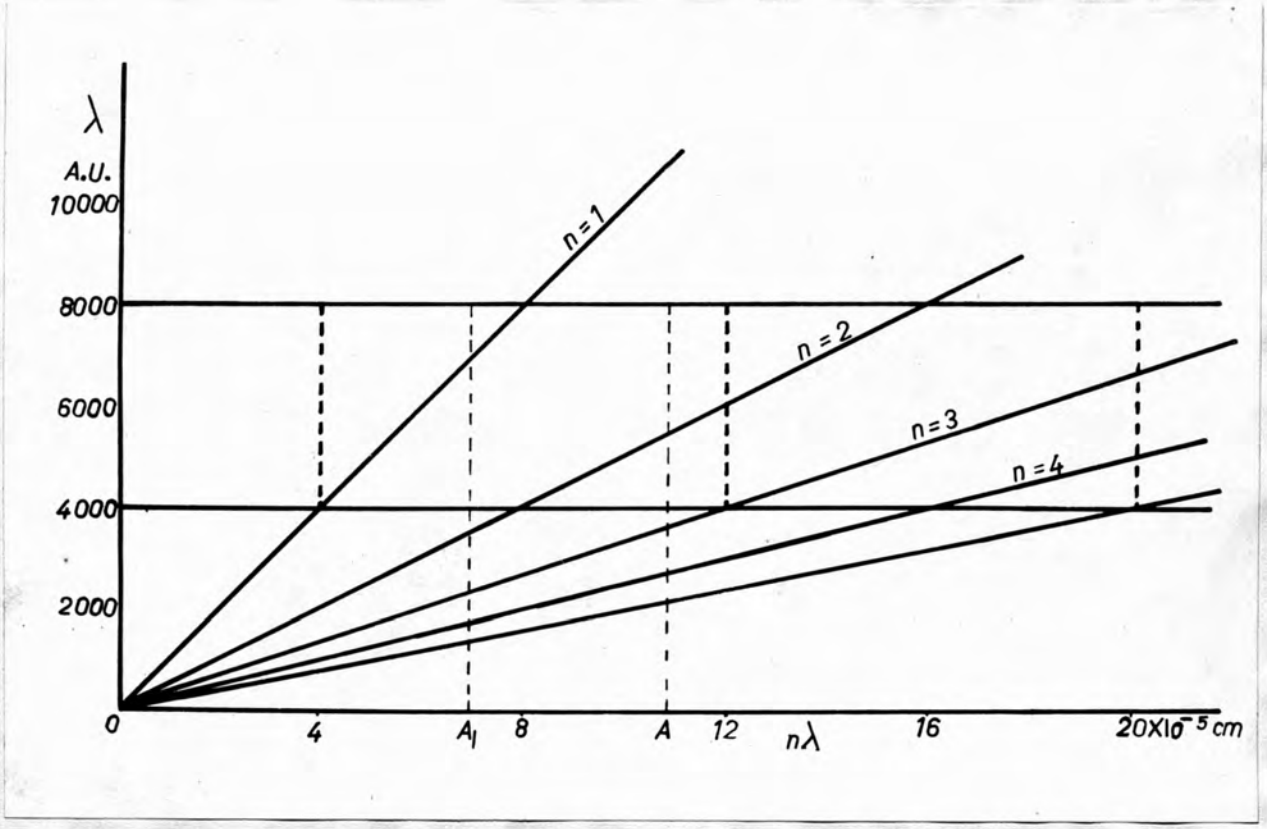
λ
A.U.
10000
8000
6000
4000
2000
n=1
n=2
n=3
n=4
0
4
A1
8
A
12
nλ
16
20X10⁻⁵cm

FIG. 16.

As the angle of incidence increases, the path difference decreases and the line x = A moves parallel to itself to x =A'. Its points of intersection with the sloping straight lines indicate the fringes present in the field of view. Thus as θ increases (a) the fringes present move towards the violet end of the spectrum, the fringes of highest order vanish and lower order fringes come into view, (b) the resulting change in λ for a certain variation in θ is greater, the smaller n is. Thus increasing the angle of incidence where one fringe is present will bring a lower order fringe (n - 1) into view, but only if the former is not the first order fringe.

From Plate (XV) there is only one fringe in the field of view at normal incidence but another fringe appears as we rotate the interferometer through a severe angle. This proves that n = 2 for the original fringe.

Substituting in the previous equation (13) the theoretical value of the differential change of phase (at $r = n_1$) and the experimentally determined value of $d\lambda$ we obtain a value for n.

Theoretical calculation of the differential change of phase

For the theory of metallic reflection, Fresnel's formulae are modified by replacing μ by a complex quantity (41). For light polarised at right angles to the plane of incidence the reflected part A of the incident amplitude is equal to $-\frac{\tan(\theta-r)}{\tan(\theta+r)}$ and for light polarised parallel to the plane of incidence $A' = -\frac{\sin(\theta-r)}{\sin(\theta+r)}$ Putting $\mu_0 - i\alpha = Me^{i\alpha}$ in the form , then μ_0 is the refractive index of the medium, i.e. the ratio of the velocity of light in air to that in the medium, and a/μ_0 is the absorption coefficient. Since $\sin\theta = \mu \sin r = (\mu_0 - ia)\sin r$ the quantity is complex and

$$\cos r = (1 - M^2 \sin^2\theta e^{2i\alpha})^{1/2} = C e^{-iu}$$

Putting $A = R e^{i\phi}$ and $A' = R' e^{i\phi'}$, then the differential change of phase $(\phi - \phi')$ between the light polarised at right angles and parallel to the plane of incidence is deduced as follows:

$$R/R' \cdot e^{i(\phi-\phi')} = \frac{\tan(\phi-r)\cdot\sin(\theta+r)}{\tan(\theta+r)\cdot\sin(\theta-r)}$$

$$= \frac{\mu\cos r\cos\theta - \sin^2\theta}{\mu\cos r\cos\theta + \sin^2\theta}$$

and since $\mu\cos r = MC e^{i(\alpha+\mu)}$ then

$$R/R'\cdot e^{i(\phi-\phi')} = \frac{MCe^{-i(\alpha+\mu)}\cos\theta - \sin^2\theta}{MCe^{-i(\alpha+\mu)}\cos\theta + \sin^2\theta}$$

$$\therefore \tan(\phi-\phi') = \frac{2MC\cos\theta\sin^2\theta\sin(\alpha+\mu)}{M^2C^2\cos^2\theta - \sin^4\theta}$$

also $Ce^{-i\mu} = \left(1 - M^{-2}\sin^2\theta e^{2i\alpha}\right)^{1/2}$

$$\therefore C^4 = 1 - 2M^{-2}\sin^2\theta\cos 2\alpha - M^{-4}\sin^4\theta$$

and $\cot 2\mu = M^2\operatorname{cosec}^2\theta\operatorname{cosec}2\alpha - \cot 2\alpha$

For a medium of refractive index μ_1 $\left(\frac{M}{\mu_1}\right)$ replaces M in the above equations and $\tan(\phi-\phi')$ is given by (42)

$$\tan(\phi-\phi') = 2\left(\frac{M}{\mu_1}\right)\frac{C\cos\theta\sin^2\theta\sin(\alpha+\mu)}{\left(\frac{M}{\mu_1}\right)^2C^2\cos^2\theta - \sin^2\theta} \quad \ldots\ldots (14)$$

where u and c are determined for any angle of incidence θ by $\cot 2\mu = \left(\frac{M}{\mu}\right)^2\operatorname{cosec}^2\theta\operatorname{cosec}2\alpha - \cot 2\alpha$

$$C^4 = 1 - 2\left(\frac{M}{\mu_1}\right)^{-2}\sin^2\theta\cos 2\alpha + \left(\frac{M}{\mu_1}\right)^{-4}\sin^4\theta$$

and $M = \left(\alpha^2+\mu_0^2\right)^{1/2}$

$$\tan\alpha = \frac{\alpha}{\mu_0}$$

The optical constants for silver in bulk as measured by Hass (43) are n = .177 K = 18.60 for λ = 5461 A. Therefore μ_0 = .177 a = 3.29. The refracture index of MgF2 μ_1 = 1.36.

The following table gives values of the differential change of phase MgF2/Ag as a fraction of wavelength, calculated from equations (14). The angle θ is the angle at which the incident light reaches the interface MgF2/Ag. It is the same as the angle r in the conditions of interference equation (12).

r°	20	30	40
$\frac{f^{\perp} - f''}{\lambda}$	.016	.039	.067

For $\hat{r} = 32^{\circ}$ d λ = 230 A at in the region of 5000 A

The theoretical value for $\left[\frac{f^{\perp} - f''}{\lambda}\right]_{r=32}$ is very nearly = .044 Substituting in equation (13), the order of interference n = 1.91 = 2 in agreement with the result of the method for the evaluation of n previously mentioned.

Section IV

Application of the fringes of equal tangential inclination to uniaxial crystals

Case of a uniaxial crystal cut perpendicular to the optic axis.

Unless travelling along the optic axis, an incident beam entering the crystal is split into two beams polarised in perpendicular planes;

(a) the ordinary ray whose electric vector is vibrating at right angles to the plane of incidence, with a constant refractive index μ_o which is independent of the direction of propagation.

(b) an extraordinary ray whose electric vector is vibrating in the plane of incidence, with a refractive index μ_e which varies with the angle of incidence. This refractive index attains a limiting value μ_e for light incident perpendicular to the optic axis, and is given by the following equation for any angle of refraction r_e

$$\frac{1}{\mu_e^2} = \frac{\cos^2 r_e}{\mu_o^2} + \frac{\sin^2 r_e}{\mu_e^2}$$

Multiply reflected rays resulting from each of the two refracted rays produce a system of interference fringes. If δ_1 and δ_2 are the path differences for the two systems, then

$$\delta_1 = 2\mu_o \, t \cos r_o$$

$$\delta_2 = 2\mu_e \, t \cos r_e$$

neglecting the deviation from the basic formula.

At the centre of the two systems, i.e. at $\theta = o$, $_e$ is equal to μ_o. Consequently no separation takes place between the members of the same order belonging to each system. As θ increases μ'_e differs steadily from μ_o and separation takes place which increases with .

Experimental arrangement.

A piece of phlogopite mica of high quality was selected, cleaved and doubly silvered. The fringes of equal chromatic order (44) were obtained as shown in Plate (XVI). No birefringence doubling effect was detected, using a constant deviation spectrograph.

This establishes that the sample of phlogopite mica can be considered to be a uniaxial crystal. The specimen was then bent in the form of a cylinder, and a parallel beam of monochromatic light was incident as previously described. The resulting fringes of equal tangential inclination are as shown in Plate (XVII).

The introduction of a nicol prism into the incident beam proved that the two systems of fringes are at right angles to each other, the outer fringes being formed by the beam whose electric vector vibrates perpendicular to the plane of incidence, i.e. the ordinary ray. The reason lies in the fact that the phlogopite mica is a negative crystal, i.e. o e. Fig. (17) represents the principal sections of the wave-surfaces of a negative uniaxial crystal, the axes being taken proportional to the refractive indices.

The difference in intensities of the fringes of the two systems as increases is due to the differential absorption for light polarised in two perpendicular planes.

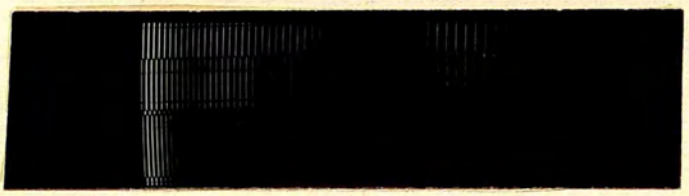

Plate. (XVI)

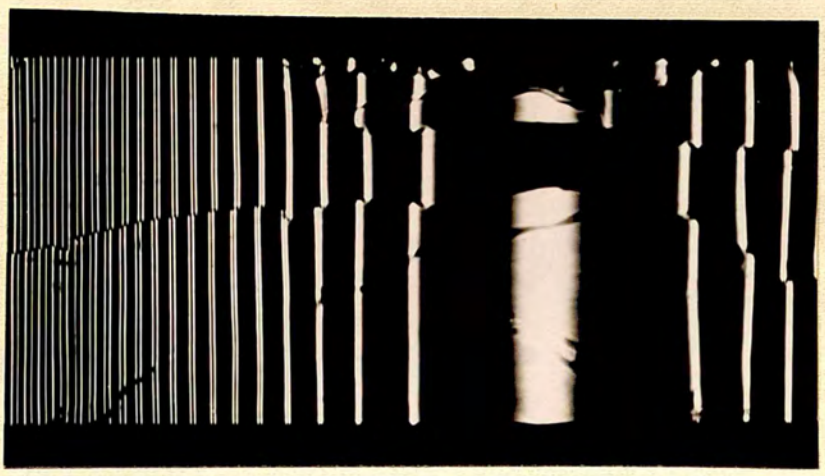

$R = 1.5$ cm

Plate. (XVII)

$t = .045$ mm

The effect of the differential change of phase at reflection for light polarised in two perpendicular planes on the separation between the fringes is discussed in the next chapter, where the uniaxial crystal is considered to be a biaxial crystal with zero optical axial angle.

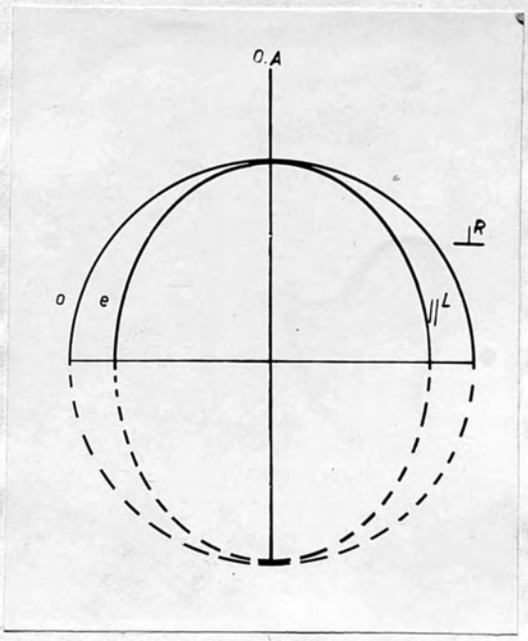

FIG. 17.

SECTION V

Application of the fringes of equal tangential inclination to biaxial crystals

Case of a biaxial crystal cut perpendicular to the acute bisectrix.

Since any ray incident on the crystal is generally split into two rays polarised in perpendicular planes and travelling with slightly different velocities and in different directions, the multiply reflected rays resulting from each of the refracted rays will produce a system of interference fringes. If δ_1 and δ_2 are the path difference for the two systems we have

$$\delta_1 = 2\mu^{1}\, t \cos r^{1}$$

$$\delta_2 = 2\mu^{11}\, t \cos r^{11}$$

where $\sin\theta = \mu^{1} \sin r' = \mu^{11} \sin r''$ μ^{1} and μ^{11} being the refractive indices for the two refracted rays for a certain angle of incidence .

Let us consider first the plane containing the optic axes. The section of the wave surface by that plane consists of a circle of radius μ_m and an ellipse

whose axes are μ_g and μ_p. For the circular section

$$\delta_1 = 2\mu_m \, t \cos r$$

and $$\delta_1^2 = 4t^2 (\mu_m^2 - \sin^2 \theta) \qquad (14).$$

For the elliptic section

$$\frac{1}{\mu 2} = \frac{\cos^2 r}{\mu 2_g} + \frac{\sin^2 r}{\mu^2_p}$$

$$= \frac{1}{\mu^2 g} - \frac{\sin^2 r}{\mu^2_g} + \frac{\sin^2 r}{\mu^2_p}$$

Hence

$$1 = \frac{\mu^2}{\mu^2_g} + \mu^2 \sin^2 r \left(\frac{1}{\mu^2_p} - \frac{1}{\mu^2_g} \right)$$

or

$$\mu^2 = \mu^2 g - \sin^2 \theta \left(\frac{\mu^2_g}{\mu^2_p} - 1 \right) \qquad (15)$$

$$\therefore \delta 2^2 = 4t^2 \left(\mu^2_g - \sin^2 \theta \left(\frac{u^2_g}{u^2_p} - 1 \right) - \sin^2 \theta \right)$$

$$= 4t^2 \left(\mu^2 g - \frac{\mu^2_g}{\mu^2_p} \sin^2 \theta \right) \qquad (16)$$

From the last three equations it is clear that there are two indendent systems of fringes polarised in mutually perpendicular planes. The first system corresponding to equation (14) is of constant refractive index μ_m and vibrates perpendicular to

the plane of incidence which is also the optical axial plane. The other system, corresponding to equations (15) and (16), vibrates in the plane of incidence with a variable refractive index u which varies with the angle of incidence as given by equation (15). The refractive index u is equal to μ_g at $\theta = o$, where $\mu_g > \mu_m > \mu_p$. As increases, μ decreases and it attains the value u_m at an incidence equal to the apparent optic axial angle E satisfying the equation sin $= \mu_p \sqrt{\frac{\mu^2_g - \mu^2_m}{\mu^2_g - \mu^2_p}}$.

It decreases further to the limiting value u_p at $\theta = \frac{\Pi}{2}$.

This means that starting from small angles of incidence the outer fringe is that vibrating in the plane of incidence, and the separation between each pair of fringes belonging to the two systems and of the same order of interference, decreases with θ until they overlap at $\theta = E$. As the angle of incidence increases beyond $\theta = E$, this separation increases, but the inner fringes now vibrate in the plane of incidence.

Let us consider the plane perpendicular to that containing the optic axes. The path differences δ_1 and δ_2 for the two systems are given by the equations

$$\delta_1^2 = 4t^2 \left(\mu_g^2 - \sin^2\theta\right)$$

$$\delta_2^2 = 4t^2 \left(\mu_m^2 - \frac{\mu^2_m}{\mu^2_p} \sin^2\theta\right)$$

The corresponding systems are again plane polarised in mutually perpendicular planes. But in this case no overlapping of any pair of fringes belonging to the two systems and of the same order of interference takes place.

Experimental arrangement

A piece of high quality, muscovite mica was selected and the plane containing the optic axes was determined by means of a polarising microscope. A thin film was cleaved and doubly silvered. It was then bent in the form of a cylinder along the direction of the intersection of the optical axial plane with the cleaved surface. The resulting fringes of equal tangential inclination are shown in Plate (XVIII).

The properties of the two systems of fringes.

(a) As predicted by theory, the separation between any two pairs of fringes of the same order of interference, decreases with θ until they overlap, and then increases again.

(b) The two systems are polarised in perpendicular planes, the outer fringe, before overlapping, corresponds to the ray vibrating in the plane of incidence. After overlapping, the inner system corresponds to this vibration direction.

(c) The angle at which the two systems overlap is not exactly equal to the apparent optical axial E of the mica crystal. It increases as the thickness of the mica film decreases. This is due to the differential change of phase at reflection mica/silver for light polarised in mutually perpendicular planes, which is to be discussed later in detail.

The associated white light fringes in transmission.

The monochromatic localized fringes of equal tangential inclination were then projected on to the slit of a spectrograph by an achromat, and a pointolite replaced the mercury arc. The resulting white light fringes in transmission are shown in Plate (XIX). Their shape illustrates more clearly the previously mentioned properties. In the case of the monochromatic system, the difference in the refractive indices of the two systems appears as a difference in angles of incidence, while in the white light fringes, the outer fringes correspond to the longer wavelengths and belong to higher refractive indices.

Select any pair of fringes of the same order of interference. Visual observation is sufficient to determine that, since the magnitude of the doubling separation due to the mica birefringence is independent of the thickness of the mica film for any fixed wavelength and is of the order of 0.004(45). In Plate (XIX) the closer pair of fringes are of the same order of interference. Now as the angle of incidence increases along the

line of the slit, starting from θ = o at the centre, the doubling separation decreases. This is due to a decrease in the difference between the two refractive indices μ_g and μ_m at a certain wavelength at normal incidence. It is clear that the refractive indices vary along each pair of fringes, with θ and with wavelength. Over a small wavelength range and for the purpose of general description, the variation of μ with wavelength is to be disregarded. Further increase in θ brings the two pairs of fringes closer, until they intersect at an angle which varies slightly with wavelength. Then the fringes diverge again. Also introducing a nicol prism proves that the component of the doublet corresponding to the longer wavelength results from the ray vibrating in the plane of incidence.

This is in accordance with the information obtained from the principal

sections of the wave-surface by the plane containing the optic axes, i.e. xz plane - shown in Fig. (18). Since a ray vibrating perpendicular to xz plane, i.e. parallel to the OY vibration-direction will spread with a velocity v_m and refractive index u_m and the corresponding section of the wave-front is a circle whose radius is proportional to v_m, or using Fletcher indicatrix (46), the radius is proportional to μ_m.

A ray vibrating parallel to the direction-vibration oz proceeds along ox with velocity proportional to v_p and refractive index u_g. As the vibration-direction moves from oz to ox, the velocity increases until it reaches a maximum value v_g when the vibration-direction becomes parallel to ox and equal to v_g with refractive index u_p. Since v_m lies between v_g and v_p, the two sections intersect at four real points which are at the extremities of the two optic axes of the biaxial crystal.

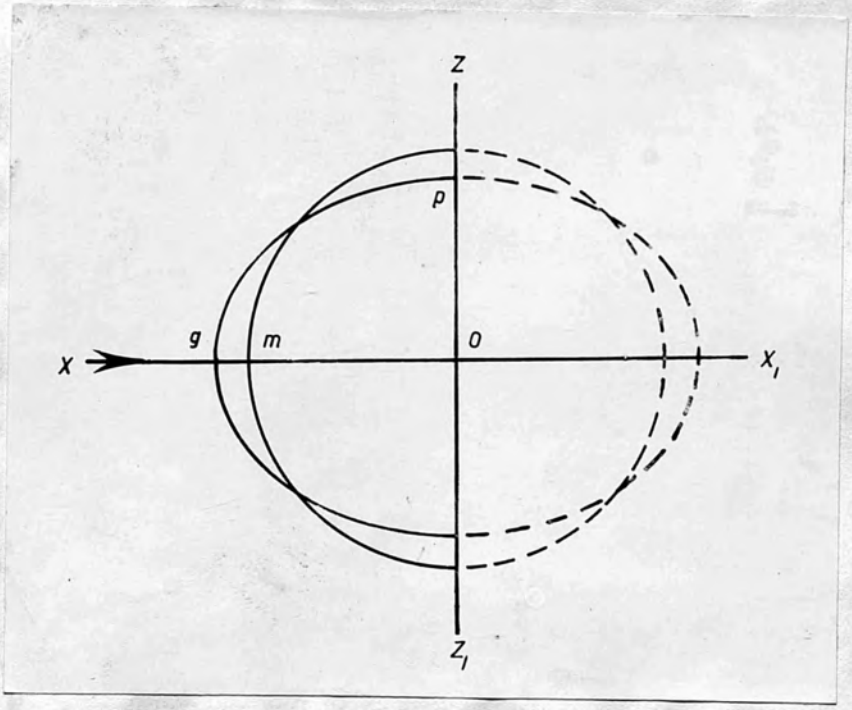

FIG. 18.

In fact these two lines are the axes of single ray velocity which differ but very slightly, in our case, from the directions of single wave velocity and single refractive index so that it is unnecessary to differentiate between them. (47).

When the specimen was bent along the perpendicular direction, the resulting two systems of fringes of equal tangential inclination are shown in Plate (XX). These two systems are also polarised in mutually perpendicular planes. Overlapping the fringes in this case does not take place between components of the same order, but if

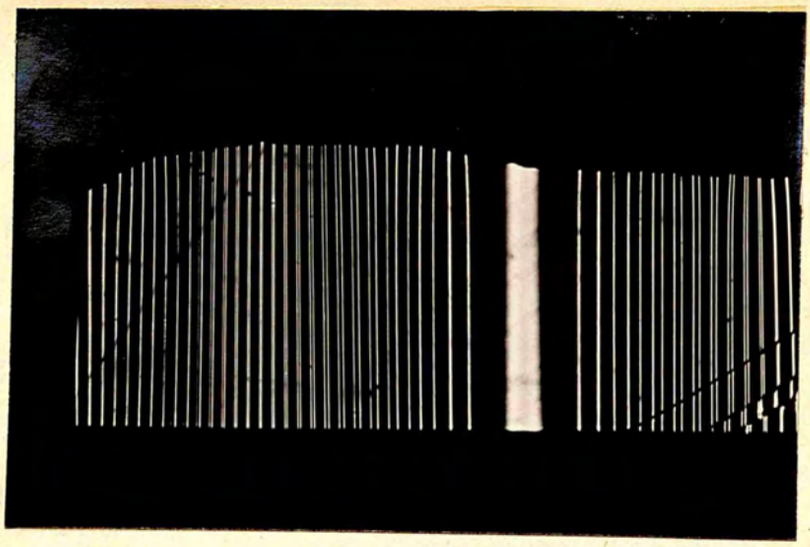

R = 1.5 cm. **Plate. (XX)** t = .030 mm

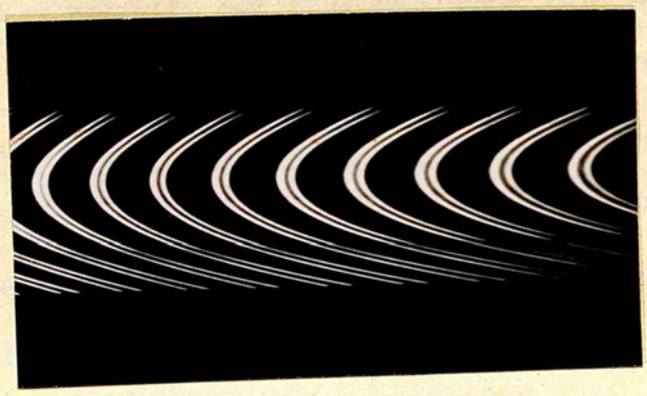

R = 1 cm. **Plate. (XXI)** t = .007 mm

it occurs as in Plate (XX), it takes place between fringes of successive orders of interference. The best way to distinguish between true and apparent overlapping of fringes is by obtaining the associated system of white light fringes in transmission as shown in Plate (XXI). The outer fringes vibrate perpendicular to the plane of incidence with a constant refractive index μ_g (neglecting the variation of the refractive index with wavelength over the wavelength-range of the fringe) for all angles of incidence. The inner fringes are vibrating in the plane of incidence with a varying refractive index with the angle of incidence θ, starting from $\mu = \mu_m$ at the centre of the system. As θ increases the separation between any pair of fringes of the same order n increases and no true intersection takes place. Either of the two fringes may intersect with one or more successive fringes depending upon the value of the thickness t of the mica sheet. The higher the value of t, the more frequent is the apparent intersections. One component intersects with higher orders and the other with lower orders.

Fig.(19) represents the principal sections of the wave-surface by the plane perpendicular to the optical axial plane, the lengths of the principal axes being taken proportional to the refractive indices.

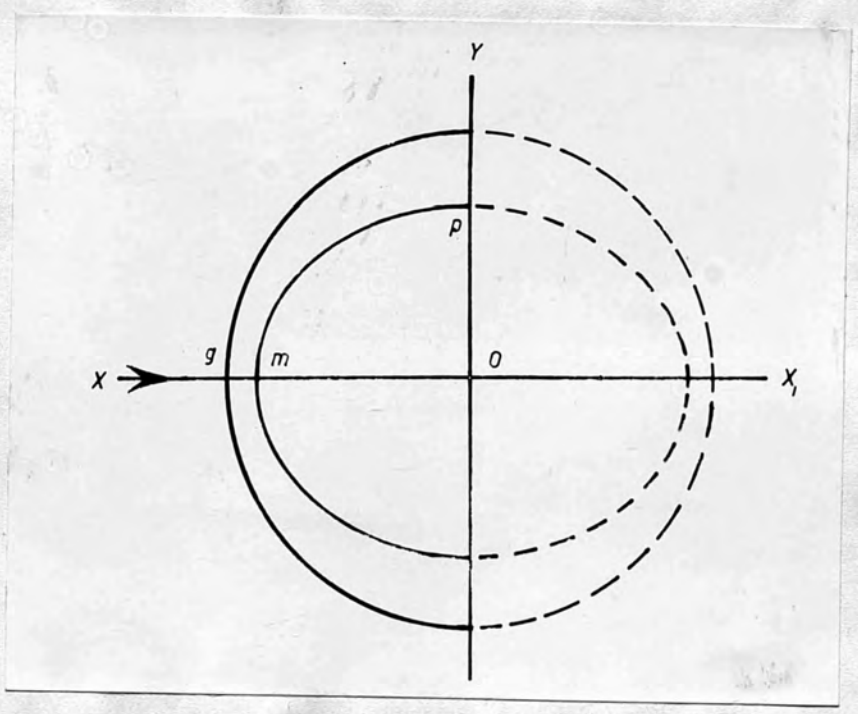

FIG. 19.

The differential change of phase at reflection mica/silver and the measurement of the optic axial angle.

Let B denote the change of phase at reflection mica/ Ag for a certain wavelength λ, angle of incidence θ and azimuth η. The condition of interference is

$$n\lambda = 2\mu t \cos r + 2\beta$$

$$\lambda\left(\eta - \frac{2\beta}{\lambda}\right) = 2\mu t \cos r$$

therefore $$\frac{\lambda^2}{4t^2}\left(n - \frac{2\beta}{\lambda}\right)^2 = \mu^2 - \sin^2\theta \qquad (17)$$

In the case of the doubly silvered mica film bent along the optical axial intersection with the plane of cleavage, and for any angle of incidence θ, an incident beam is split into two beams polarised in two mutually perpendicular planes. The beam vibrating perpendicular to the optical axial plane, which is the plane of incidence, has

a constant refractive index μ_m independent of θ. If $B_{\underline{1}}$ denotes the corresponding change of phase at reflection at a certain angle θ, then

$$\frac{\lambda^2}{4t^2}\left(n - \frac{2\beta_{\underline{1}}}{\lambda}\right)^2 = \mu_m^2 - \sin^2\theta \qquad (18)$$

For light polarised in the perpendicular plane, its refractive index μ satisfies equation (15) as θ varies. At $\theta = E$, the apparent optic axial angle, μ is equal to μ_m and consequently the corresponding members of the same order of interference n ought to overlap. But, because of the difference between $B_{\underline{1}}$ and B^{11}, the latter is the change of phase at reflection of the beam vibrating in the plane of incidence, the separation between the fringes is not zero at $\theta = E$.

For the second system, equation (17) becomes

$$\frac{\lambda^2}{4t^2}\left(n - \frac{2B^{11}}{\lambda}\right)^2 = \mu_o^{1\,2} - \sin^2\theta \quad (19)$$

At the angle of overlapping θ_1, the effect of the difference in the refractive indices of the two systems, on the position of the fringes, i.e. the separation between them, has equalised but with an opposite sign to the corresponding effect due to the difference in the phase changed $(\beta^{11} - \beta^{\perp})$. at $\theta = \theta_1$ we have

$$\frac{\lambda^2}{4t^2}\left\{n - \frac{2B^{\perp}}{\lambda}\right\}^2 - \mu_m^2 = \frac{\lambda^2}{4t^2}\left\{n - \frac{2B^{11}}{\lambda}\right\}^2 - u_{\theta_1}^2$$

where B and B^{11} correspond to $\theta = \theta_1$

$$\frac{\lambda^2}{4t^2}\left\{\left(n - \frac{2B^{\perp}}{\lambda}\right)^2 - \left(n - \frac{2B^{11}}{\lambda}\right)^2\right\} = u_m^2 - u_{\theta_1}^2$$

$$\text{hence}\left(B^{11} - B^{\perp}\right) = \frac{\mu_m^2 - u_{\theta_1}^2}{\left(n - \frac{B^{\perp} + B^{11}}{\lambda}\right)} \cdot \frac{t^2}{\lambda^2}$$

and to a very close approximation

$$\left(\frac{B^{11} - B^{\perp}}{\lambda}\right) = \frac{u_m^2 - u_{\theta_1}^2}{\theta = \theta_1\sqrt{u_m^2 - \sin^2}} \cdot \frac{t}{2\lambda} \quad (20)$$

The last equation shows the dependence of the angle of overlapping on the thickness t. As θ_1 tends to E, $\mu(\theta_1) \rightarrow u_m$, but since $\left(\frac{B^{11} - B^{\perp}}{\lambda}\right)$ at $\theta = E$ or $r = V$ has got a finite value, then the thickness t should tend to infinity. In other words, the higher the value of t, the nearer θ_1 is to E. This is in accordance with experimental observations.

For the case of phlogopite mica considered as a uniaxial crystal, it is clear that the effect of the differential change of phase is to bring the two systems closer to each other.

It is important to mention that exact overlapping does not always take place. Also in many ways we are left with a region of overlapping. These limit the degree of accuracy of measuring θ_1.

No if θ, θ_2 and $_2$ are the two angles of overlapping corresponding to the thickness t_1 and t_2 of the same specimen, then by calculating theoretically the values of $\left(\frac{B^{11} - B^{\perp}}{\lambda}\right)$ for the two

angles r_1, and r_2 at which the incident light reaches the mica/silver interface, then μ (θ_1) and μ (θ_2) can be obtained, knowing μ_m. (Equation (21)

Substituting for μ (θ_1) and μ (θ_2) in

$$\mu^2 \ (\theta) = \mu^2_g - \sin^2\theta \left(\frac{\mu^2_g - 1}{\mu^2_p} \right)$$

the values of μ_g and μ_p are deduced. Substituting in the equation

$$\sin = \mu_p \sqrt{\frac{\mu^2_g - \mu^2_m}{\mu^2_g - \mu^2_p}}$$

the angle E can be determined.

Results:

For high quality australian muscovite mica

$\theta_1 = 35^\circ \ 30'$ $\qquad$ $t_1 = .033$ mm.

$\theta_2 = 34^\circ$ $\qquad$ $t_2 = .039$ mm.

$\left[\frac{B^{11} - B^{\perp}}{\lambda}\right]_{r_1 = 21^\circ 30'} = .0195$

$\left[\frac{B^{11} - B^{\perp}}{\lambda}\right]_{r_2 = 20^\circ 30'} = .0190$

$\mu_m = 1.59 \quad \mu_g = 1.595 \quad \mu_p = 1.56$

$E = 33^{\circ}\ 12'$

The value determined by the writer for E using high quality muscovite mica is in close agreement with the values given by Tutton (48) (30° - 37°), P fund (49) (33) and Chinmayanandam (50).

Chapter VI

Evaporation Technique

Equipment Used

The thermally evaporated films of silver and magnesium fluoride used were produced in the evaporation plant shown in plate (XXII). It is a commercial coating unit type E3 manufactured by W. Edwards & Co. This plant is of the vertical type. The vacuum chamber is a large pytex bell-jar, 60 cms high, resting on a massive steel baseplate, a vacuum seal being made by an ungreased rubber gasket on the lower edge of the bell jar. A large diameter valve set into the baseplate connects the chamber to a three stage oil diffusion pump. Two vacuum tight insulated electrodes are fastened into the baseplate, the third is earthed. The evaporation filaments are connected between the electrodes. The substrates to be coated are placed on a table, same 30 cms above the filament. A movable shutter is placed between the filament and substrate.

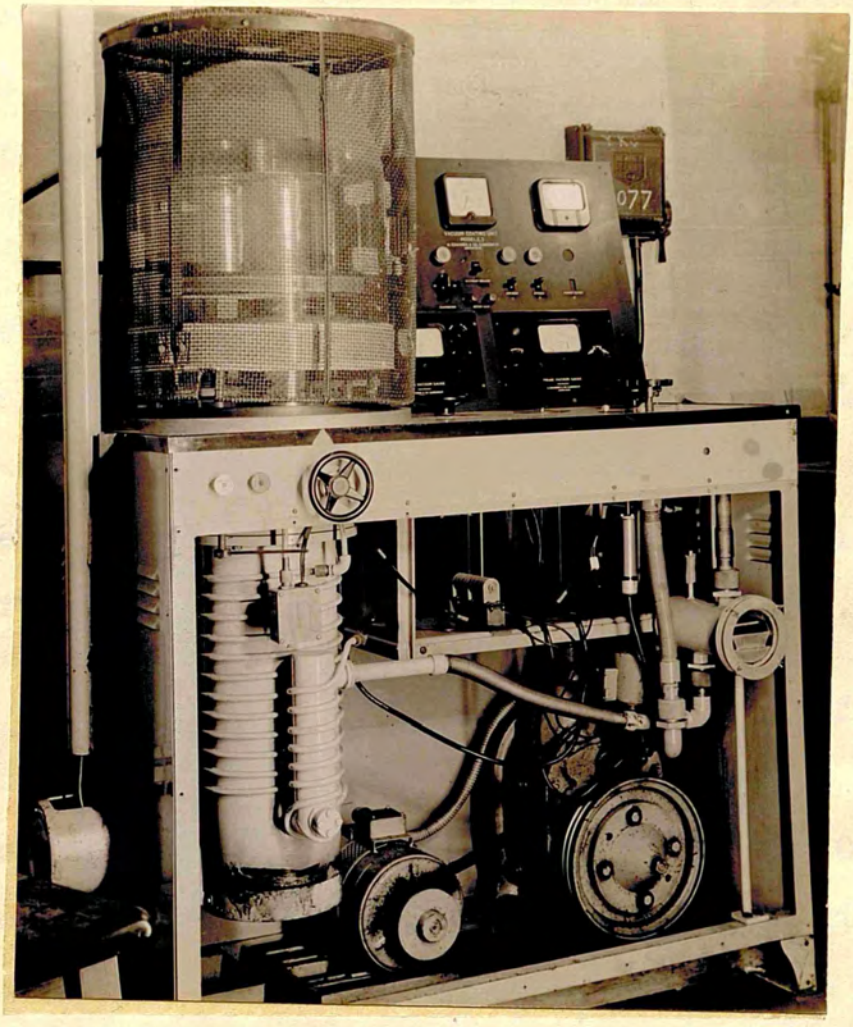

Plate. XXII.

The voltage available for passing a high tension discharge between two rings situated between the filament and the specimen table is 3,300 V. The maximum filament heating current available is 150 amps.

The capacity of the bell jar and speed of the pump are such that a complete evaporation process in case of silver using one filament only takes half an hour. In the case of magnesium flurode a longer time is needed since two filaments are usually used successively.

The pressure in the chamber is measured by a Philips type ionization gauge, a cold cathode gauge. The evaporation is below 10^{-4} mms of mercury, but the gauge does not permit any accurate estimation of pressure of this order. Plate (XXIII) is showing the arrangement of the components on the baseplate:

The evaporation procedure:

The substrates used in this work were

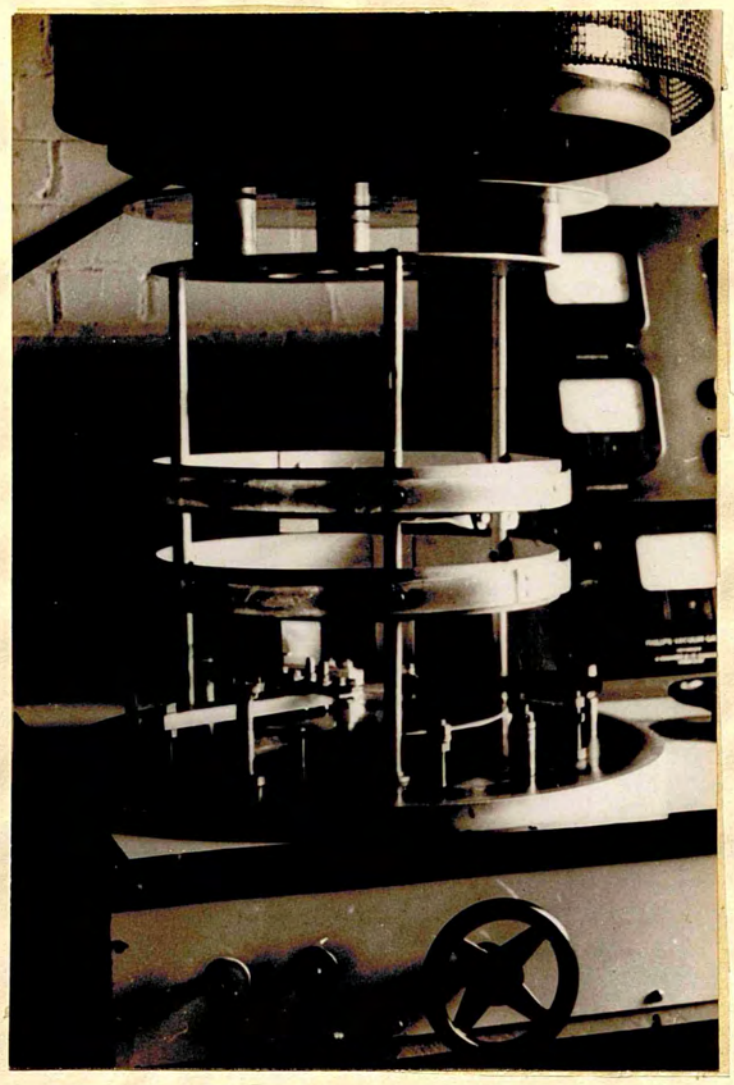

Plate. XXIII.

either optical glass flats and lens or mica sheats. The glass substrates are washed with nitric acid or hydrogen peroxide, then rinsed with tap water and dried with cotton wool. The surface is considered satisfactorily clean when breathing produce a uniform film which disappears in a second or less. Freshly cleaved mica surfaces are quite clean and require no treatment other than degassing in a vacuum. The substrate is then placed in the evaporation chamber and when a fairly good vacuum is reached, air is admitted to a pressure of a few millimeters of mercury, and a high tension discharge is passed in the chamber to clean the specimen further by ionic bombardment for 5 - 10 minutes before pumping was resumed. About 250 milliamps pass in the discharge at 1500 volts. The pressure is now reduced by the diffusion pump, and before evaporation starts, the filament is heated with the shutter over it to protect the

substrate. Any impurities are burnt off and thus prevented from reaching the surface. The shutter is removed after heating the filament for half a minute and deposition begins. Evaporation is carried out at a pressure below 10-4 mms. The filament used is a strip of molybdenum, of dimensions 6 X 1.5 cms, with a small depression in its centre.

Silver: The metal was availabe in the form of 3 mm. diameter wire, spectroscopically pure, and was evaporated in molybdenum filaments as described. The heating current was 120 amps. an opaque layer could be easily formed in 30 - 45 seconds.

The reflectivity of the silver layer can only be roughly estimated during evaporation by looking through it at the heated filament. Such visual estimation can only lead to an approximate estimation especially when substates

of different thickness are used, like mica sheets.

Magnesium fluoride; it is available in the form of pure white powder. Molybdenum filaments are used and gradual heating is essential otherwise the powder sputters. A maximum current of 90 amps. was found to be convenient.

Uniformity in the thickness of evaporated layers;

Under perfect conditions of vacuum there still remainsthe question of obtaining a layer of uniform thickness. It is apparent that in the case of evaporation to the inside surface of a sphere from a point source, a film of uniform thickness is obtained. For a plane surface, if D is the density at a point for which the angle between the normal to the plane and the line joining the point is ψ , then $D = d \cos^3\psi$, d being the density at the normal projection of the source on the surface.

In this evaporation plant, the separation of the source and the substrate is 30 cms. The density at the circumference of a circle of 1 cm. radius on the substrate in therefore less than that at the centre by about 1% Tolansky (51). This is improvized in practice since the filament is an extended source.

A slight difference in thickness has been detected in the case of magnesium fluoride films of more than a wavelength in thickness at two points more than 3 cms apart, with the result of bending the fringes of equal chromatic order.

Influence of conditions of evaporation:

(1) A marked increase of reflectivity was detected by increasing the speed of evaporation according to Sennett & Scott (52).

(2) Vacuum Condition:

The degree of vacuum required for successfully carrying out the process of evaporation is such that the mean free path of the molecules leaving the metal is greater than the greatest distance between the source and the substrate (53).

Influence of surface conditions:

(1) Imperfect cleaning is no doubt the cause of too low values of R.

(2) Indirect measurements of the reflectivity of silver films (54) by measuring the width of interference fringes produced with etalons of very small spacing showed that the imperfection of the etalon plates had an effect which becomes more important as R increases.

Reflectivity and absorption of silver films:

Among the early workers who carried out direct measurements of reflectivity of silver films are Goos (1936) (55) and Rouard (1937) (56) Krautkramer (1938) (57). The first two workers were concerned with silver films resulting from sputtering. The measurements of Krautkramer fall into the region of high reflectivities. He used a mercury diffusion pump and the resulting pressure was of the order of 10^{-5}mm Hg.

The work of Strong and Dibble (1940) (58) was mainly confined to the range of low and medium reflectivity. They reported the existence of two different types of silver films below a certain thickness

The values of R and A used in calculating the maximum and minimum intensities in the transmitted and reflected systems in Chapter I

were given by Tolansky (59) and they are tabulated as follows:-

R	60	70	75	80	85	90	94
T	35.5	27	22	16.5	10.5	4.5	.7
A	4.5	3	3	3.5	4.5	5.5	5.3

Kuhn & Wilson (1950) (60) using a mercury diffusion pump and a liquid air trap at pressure of 3 - 5 X10-5 mm of Hg, measured the values of R and T in the range of high reflectivity. The values of R were reported to be nearly always found to lie close to a standard curve giving R as a function of T, the wavelength and the age of the film. Their values are in agreement with the previous data given by Krautkramer.

The values of R and T as calculated from the standard curve for new films are as follows:

(λ = 5200 A.)

R	84	88	90	92	96
T	12.6	9.2	7.4	5.7	2
A	3.4	2.8	2.6	2.3	2

It is certain that the reflectivity decreases with age and more rapidly for shorter wavelengths.

REFERENCES.

(1) Tolansky, Multiple-beam interferometry of surface and thin films (1948)

(2) Airy, Math.Tracts, p.381 (1831)

(3) Boulouch, J. de Physique, 5,789 (1906)

(4) Fabry and Perot, Ann.de Chim.et de Physique, 12,459 (1897)

(5) Tolansky, see reference (1)

(6) Tolansky, Physica, 12,649 (1946)

(7) Hamy, Phys. Rodium, 5,789 (1906)

(8) Holden, Proc.Phys. Soc.,B,62,405 (1949)

(9) Brossel, Proc.Phys.Soc., 59,226 (1947)

(10) Tolansky, see reference (1) p.18-20

(11) Pahlen, Gehrcke's Handbuck der Physik Optik Vol I (1927)

(12) Feussner, Gehrcke's Handbuck der Physik Optik, Vol I (1927)

(13) Brossel, see reference (9) p.230

(14) Tolansky, Proc.Roy.Soc. A ,184,51 (1945)

(15) Baly, spectroscopy p.59 vol 1. (1927)

(16) Morris, M.Sc. Thesis Manchester University (1946)

(17) Tolansky, see reference (1) p.104.

(18) Khamsavi and Donaldson, Nature, 159,228 (1947)

(19) Avery, Nature, 163,916 (1949)

(20) Faust, Phil. Mag., 41, 1240 (1950)

(21) Rouard, Ann. de Physique, 7,291 (1937)

(22) Barakat, Nature, 16, 603 (1949)

(23) Tolansky, see reference (1) p.109

(24) Griffin, Ph. D. Thesis London University (1950)

(25) Raman and Rajagopolan, J.O.S.A., 29,413 (1939)

(26) Raman and Rajagopolan, Proc. Ind. Acad. Sci, 10, 317 (1939)

(27) Tolansky and Barakat, Proc. Phys. Soc. 63,545 (1950)

(28) Hardinger, Pogg. . Ann. 77,217 (1849)

(29) Hansen, Gehrcke's Handbuck der Physik Optik (1927)

(30) Bond, Phil. Mag. 16,410 (1933)

(31) Tutton, Crystallography and practical crystal measurements, vol I, p.523 (1922)

(32) Tolansky, see reference (1) p.24

(33) Bunn, Chemical crystallography p.63-65 (1946)

(34) Eisner, Research, 183 (1951)

(35) Fabry and Perot, see reference (4)

(36) Tolansky, see reference (1) p.58

(37) Greenland, J. Mic.Soc. sep.(1949)

(38) Tolansky, see reference (1) p.41

(39) Donaldson, PH.D. Thesis,Manchester University (1946)

(40) Tolansky, see reference (1)(p.163).

(41) Wood, Physical Optics, p.547 (1934)

(42) Maclaurin, the theory of light I, p.241-250 (1908)

(43) Hass, Ann. der Phys., 31,245 (1938)

(44) Tolansky, see reference (1) p (126)

(45) Tolansky, see reference (1) p 115-116

(46) Fletcher, Min.Mag., 44 (1891)

(47) Dale, The form and properties of crystals p.132 (1932)

(48) Tutton, see reference (31) p.525

(49) Pfund., J.O.S.A., 32 (1942)

(50) Chinmayanandam, Phil.Mag. (1919)

(51) Tolansky, High resolution spectroscopy p.121 (1947)

(52) Senett and Scott, J.O.S.A., 30,431 (1950)

(53) Dunoyer, Compt. Rend.,202,474 (1936)

(54) Bright, Jackson and Kuhn,Proc.Phys.Soc., 62,225 (1949)

(55) Goos, Z. Phys., 100,95 (1936)

(56) Rouard, Ann. de Physique, 7,291 (1937)

(57) Krautkramer, Ann. der. Phys. Lpz., 5,32, 537 (1938)

(58) Strong and Dibble, J.O.S.A., 30,431 (1940)

(59) Tolansky, see reference (6)

(60) Kuhn and Wilson, Proc.Phys.Soc., 63,745 (1950)

ACKNOWLEDGEMENT .

The writer is very grateful to Professor S. Tolansky for his continuous interest, encouragement and helpful guidance throughout this work.

He also expresses his thanks to his collagues and to the workshop staff for their kind assistance.

The present work was made possible by a scholarship from the Egyptian Government, and the author is greatly indebted to Professor M. El. Sherbini for his help in this respect.